Increasing the throughput of protein-small molecule hybrid construction and evaluation on the yeast surface

A thesis submitted by

Marina Rueda Garcia

in partial fulfillment of the requirements for the degree of

Master of Science

in

Bioengineering

Tufts University

August 2022

Adviser: James Van Deventer

Committee: Joshua Kritzer, Emmanuel Tzanakakis

Abstract

Bioconjugation techniques enable the production of hybrid protein-small molecule constructs that harness the selectivity of antibodies and the potency of small molecule warheads. The vast combinatorial space of hybrid constructs calls for a high-throughput method in which a wide range of constructs can be evaluated without sacrificing bioconjugation yield or quality. This work describes a plate-based approach to performing copper-catalyzed azide-alkyne cycloaddition (CuAAC) that allows for the screening of hundreds of yeast-displayed protein-small molecule hybrids in a single day. This approach utilizes protein containing noncanonical amino acids (ncAAs) displayed on the yeast surface that contain reactive groups capable of undergoing CuAAC. In-depth assessment of reaction quality comparing reactions conducted in tubes versus 96-well plates revealed that reactions performed in plates are indistinguishable from reactions performed in tubes. This includes both high extent of reaction and no detection of carryover between samples, enabling significantly increased bioconjugation throughput (from 20-30 reactions to greater than 100). A set of six yeast-displayed fibronectins that function as hybrids were used as a model system to further investigate the utility of plate-based conjugation strategies. We performed proof-of-concept evaluating CuAAC reaction conditions and assessing binding of hybrids to human carbonic anhydrase II, utilizing more than 100 distinct reactions in each study. We found that the CuAAC reaction is flexible, yielding high extent of reaction in a wide range of conditions, and the human carbonic anhydrase binding assay led to the discovery of a new hybrid binder. Our results indicate that plate-based conjugations will greatly improve the throughput of hybrid construction and evaluation in the laboratory and aid in the discovery of potential hybrid constructs that inhibit or bind challenging targets with high specificity.

Table of Contents

Chapter 1: Introduction *6*

Bioorthogonal reactions 6

Copper-Catalyzed Azide-Alkyne Click Chemistry (CuAAC) 7

Protein-small molecule hybrids 9

Noncanonical amino acids 10

Encoding noncanonical amino acids in protein 11

Yeast Display 12

Hackel Lab work: fibronectins and carbonic anhydrases 12

Huang et al.'s work with fibronectins 13

Thesis work 14

References 17

Chapter 2: Materials and Methods *22*

Media and plate preparation 22

Buffers 22

DNA cloning and transformation, and TAG codon introduction 22

Yeast transformations 25

Noncanonical amino acid preparation 25

Cell culture and induction 26

Copper-catalyzed azide-alkyne cycloaddition click chemistry 27

Cell Sample Preparation....27
Reagents....28
Two-step CuAAC on a Plate....29
Two-step CuAAC in Tubes....30
Human Carbonic Anhydrase II Binding Assay....30
Flow Cytometry Labeling....31
Primary Labeling....31
Secondary Labeling....32
Flow cytometry....32
Extent of reaction calculations....33
References....34
Chapter 3: Results and Discussion....35
3.1. Assessing the quality of CuAAC performed in plates....35
Introduction....35
Results and Discussion....40
Conclusion....43
3.2. Mapping the CuAAC reaction landscape....44
Introduction....44
Results and Discussion....46
Conclusions....54
3.3. Human Carbonic Anhydrase II Binding Assay....56
Introduction....56
Results and Discussion....61

Conclusions 65

References 67

Chapter 4: Conclusions and future work 70

Chapter 1: Introduction

Bioorthogonal reactions

Bioorthogonal reactions take place between functional groups that react with each other selectively but do not react with surrounding biomolecules or interfere with biochemical processes under physiological conditions[1]. In the past three decades there has been an effort to design and improve these reactions for a wide variety of applications, including the visualization, characterization and bioconjugation of biomolecules such as proteins, glycans, lipids or nucleic acids[2]. Bioorthogonal reactions involve groups not typically present in biological systems and must occur at physiological temperature and pH in a fast manner, forming a stable reaction product. There are two main components of a biorthogonal reaction: (1) a biomolecule functionalized with a biocompatible functional group, and (2) a complementary probe that reacts with this functional group, which can be tagged for affinity or visualization[3]. The criteria for the complementary probes are stringent, as it must not perturb the biomolecules' environment while being robustly reactive with its target. Some of these probes include azides, terminal alkynes, ketones and aldehydes, alkenes and tetrazines, which are used in well-studied biorthogonal such as Staundiger ligations, strain-promoted azide-alkyne cycloadditions (SPAAC), inverse electron-deman Diers-Alder (IED-DA), tetrazine ligations, or photoinducible reactions[4]. Bioorthogonal chemistry allows for the characterization of complex biological environments and production biological conjugates. This work focuses on a specific type of bioorthogonal reaction, copper-catalyzed azide-alkyne cycloadditions, to produce and screen a vast combinatorial space of protein-small molecule hybrids on the yeast surface.

Copper-Catalyzed Azide-Alkyne Click Chemistry (CuAAC)

The copper-catalyzed azide-alkyne cycloaddition is a biorthogonal reaction that has been used extensively for the bioconjugation of molecular species. CuAAC involves the ligation of an azide-containing cargo with an alkyne-containing biomolecule or viceversa[5]. Azides are widely used in biorthogonal reactions because of their absence from biological systems and stability[3]. While terminal alkynes are found in a few biosynthetic pathways[6], they are nevertheless compatible with the cellular environment and react selectively with azides. Both azides and alkynes are relatively small, and they do not engage in acid-base, hydrophobic and π-stacking interactions, or hydrogen bonding with biomolecules[5]. The uncatalyzed 1,3-dipolar cycloaddition of azide and alkyne to form 1,4- and 1,5- regioisomers of 1,2,3-triazoles[7], was extensively studied by Huisgen et al.[8] but is too slow for biological purposes (Figure 1.1A). However, the addition of copper(I) as a catalyst significantly accelerates the reaction rate, making CuAAC an attractive option for biorthogonal reactions since its discovery in 2002 by Tornoe et al.[9] and Rostovtsev et al.[10]. CuAAC reactions yield a 1,4-disubstituted 1,2,3-triazole product (Figure 1.1B) that cannot be cleaved by hydrolysis and is not susceptible to oxidation or reduction but can associate with biological entities through hydrogen bonding[11].

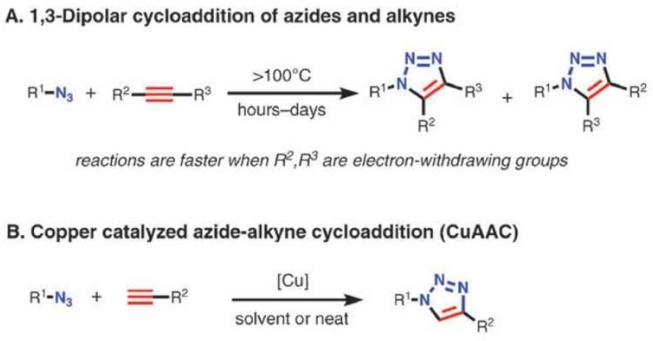


Figure 1.1. A) Uncatalyzed azide-alkyne cycloaddition. B) Copper catalyzed azide-alkyne cycloaddition. Figures from [12].

The current understanding of the CuAAC reaction mechanism[13] is represented in Figure 1.2. The reaction is initiated when the terminal alkyne forms an acetylide that engages in σ- and π-bonding with the copper(I) catalyst (S5A) and interacts with the azide to form a ternary complex (S5B). Then, a metallacycle formation takes place, and one copper(I) gets oxidized to copper (III) (S5C), and a reductive ring contraction leads to the formation of a copper (I) triazolide (S5D). The triazolide deprotonates an alkyne, completing the reaction and obtaining the 1,2,3-triazole product.

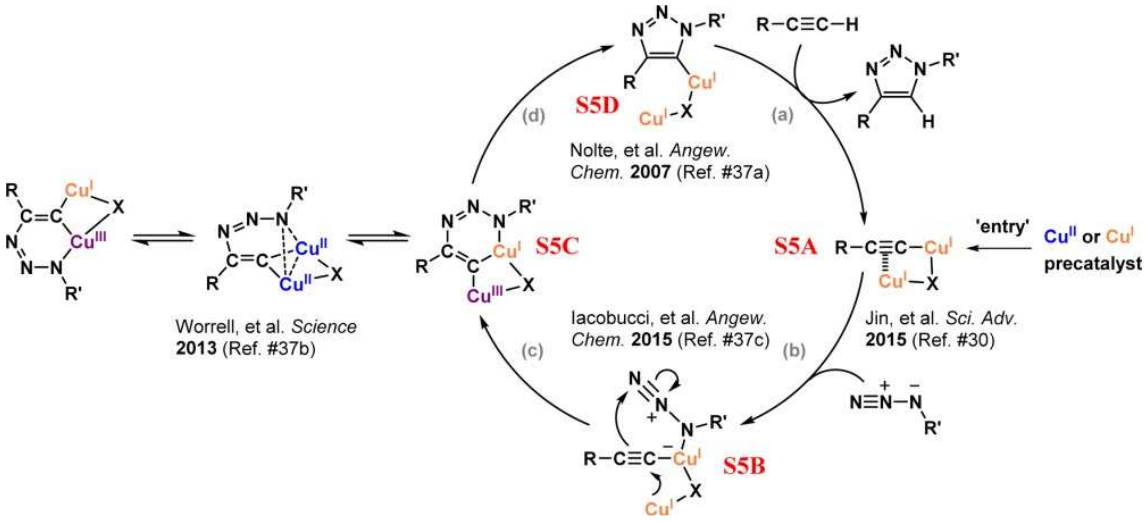


Figure 1.2. Current understanding of CuAAC reaction mechanism. Figure from [13].

Copper(I) oxidizes to copper(II) in aerobic conditions so in order to maintain the ion in its +1 oxidation state, ascorbate is used as a reducing agent as well as a copper chelating-ligand. Hong et al.'s[5] protocol recommends the use of tris(3-hydroxypropyltriazolyl-methyl)amine (THPTA) as a ligand, which shields the biomolecules from Cu(II)-mediated hydrolysis, intercepts O_2/Cu/ascorbate radicals and peroxides that could oxidize protein residues, and accelerates the reaction by maintaining a sufficient Cu(I) concentration in solution. While THPTA is a robust ligand, other poly(triazolylmethyl)amine ligands with substituent *tert*-butyl groups such as 2-[4-

{(bis[(1-*tert*-butyltriazolyl)methyl]amino)methyl}-triazolyl]acetic acid (BTTAA), 2-[4-{(bis[(1-*tert*-butyltriazolyl)methyl]amino)methyl}-triazolyl]ethyl hydrogen sulfate (BTTES) or {3-[4-({bis[(1-*tert*-butyltriazolyl)methyl]amino}methyl)-triazolyl]propyl}trimethylammonium (TABTA) are also used commonly in CuAAC reactions[14]. Wu et al. found that the reaction acceleration rate correlated with the number of sterically hindered functional groups[15]. Hong et al.'s protocol also proposes the use of aminoguanidine to suppress side reactions between arginine side chains and dehydroascorbate[5].

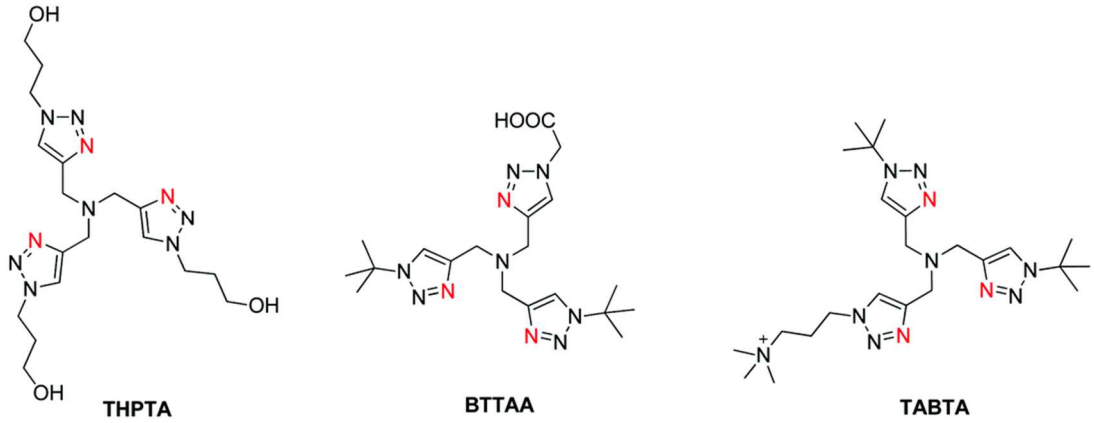


Figure 1.3. Common CuAAC copper-chelating ligands. Figure from [14].

Protein-small molecule hybrids

In recent years, protein-drug conjugates have become increasingly popular as they harness the specificity of proteins to guide small molecules to the desired target. The conjugation of small molecules to proteins can be site-specific or non-specific. For the latter, interchain disulfide bridges or surface lysine residues are usually the protein residues onto which the drug molecules are linked. The linkage occurs after reduction of either residue, but the obtained hybrids are

heterogeneous, which leads to low stability, and in the case of potential pharmaceutical products, safety concerns due to the unpredictability of the therapeutic window when administrating the pharmaceutical product[18]. Because of this, site-specific conjugation is the preferred method of conjugation to achieve homogeneous hybrids[19]. For example, cysteine residues engineered to be more reactive replace other residues in the heavy chain and act as a predefined conjugation site for the drug. Another mechanism for site-specific conjugation is to use enzyme-mediated conjugation, in which specific enzymes catalyze the conjugation reaction between the antibody and the linkers. This can be done by engineering the antibodies to include tags, such as peptide tags, glutamine, aldehydes, or ketone reactive groups[20].

Noncanonical amino acids

The genetic codes of all organisms consist of the same 20 amino acids, plus the rarely occurring pyrrolysine and selenocysteine. These canonical amino acids (cAAs) are usually functionalized through cofactors or posttranslational modifications to obtain desired chemical properties. This has inspired the development of noncanonical amino acids, which increases the variety of "building blocks", providing novel functionalities to proteins and expanding their chemical, physical and biological properties. Noncanonical amino acids (ncAAs) offer a powerful platform for site-specific incorporation of drugs onto proteins by expanding the genetic code. Engineered orthogonal tRNA/aminoacyl tRNA synthetase pairs allow for the incorporation of ncAAs with advantageous new physical, chemical, and biological properties[21]. Some of these ncAAS contain functional groups that can be linked to the small molecule of interest using biorthogonal reactions such as CuAAC. Hundreds of ncAAs have been encoded and expressed in biological organisms by exploiting the protein expression machinery[22]. Some ncAAs possess

unique fluorescent[23] or spectroscopic[24] properties that allow the study of protein expression and conformation. Photocaged ncAAs such as photocaged tyrosine and lysine can be activated by light, controlling the activity of proteins in live cells[25]. Other ncAAs contain functional groups with biorthogonal reactivity, which can be used to site-specifically conjugate drugs, polyethylene glycols, probes, or other proteins of interest[23].

Encoding noncanonical amino acids in protein

There are several methods utilized to incorporate a ncAAs to proteins expressed on prokaryotes and eukaryotes, and these strategies can be residue-specific or site-specific. Residue-specific incorporation entails adding a ncAA that resembles the structure of a cAA in addition to cAAs during protein induction[26]. The endogenous protein translation machinery will then code the ncAA, partially replacing the analog cAA. On the other hand, in site-specific incorporation of ncAAs , a codon that does not usually code for an amino acid is repurposed to encode for a ncAA. The most common methodology is stop codon suppression at the TAG (amber codon), TGA (opal codon) or TAA (ochre codon)[27]. The expression of ncAAs in this work is achieved with amber codon suppression, where an orthogonal translation machinery is expressed in the cell to facilitate the new codon readout and incorporation of the desired ncAA. Orthogonal translation systems are composed of an aminoacyl-tRNA synthetase (aaRS), which attaches the ncAA onto its cognate tRNA with the anticodon to the suppressed amber codon[28]. The ncAA-charged tRNA is then moved to the ribosome by the elongation factor-Tu, where it reads the assigned amber codon on mRNA, which leads to the incorporation of the ncAA onto the protein. The aaRS/tRNA pairs, called orthogonal as they do not interact with endogenous aaRS/tRNA pairs, must outcompete cellular release factors that are designed to terminate translation[29].

Yeast Display

Display technologies are an effective tool for protein engineering, with bacteria and yeast display platforms being the most popular, and proteins are expressed on the host cell surface and can be screened with high throughput methods[30]. Yeast display is advantageous as it allows the expression complex proteins thanks to its eukaryotic protein folding mechanism, and flow cytometry and FACS can be used to assess antigen binding to the protein being displayed. A potential disadvantage of yeast display systems is the slower culture growth and separate protein induction compared to bacterial display. Nevertheless, yeast display libraries have been used to obtain high affinity and specificity binders to antigens of therapeutic relevance such as T cell receptors[31] or botulinum neurotoxin[32]. Most proteins displayed on the yeast surface use the Aga1-Aga2 display technology developed by Wittrup et al.[33], in which the protein is fused to yeast agglutinin protein Aga2, controlled by a galactose-induced promoter. Aga2 is attached to Aga1 through disulfide bonds, and Aga1 is covalently bound to the cell through glycan linkages. Usually, the N-terminus of the protein is fused to Aga2, and epitope tags can be added to the displayed protein to harness fluorescent detection of the proteins or remove truncated proteins. Previous work by Van Deventer et al. has demonstrated that the yeast surface is a robust platform for bioconjugation harnessing ncAAs expressed on display proteins[34].

Hackel Lab work: fibronectins and carbonic anhydrases

One impressive example of the use of yeast display for protein-small molecule hybrid construction is the work done by the Hackel Lab at the University of Minnesota. Hackel et al.discovered fibronectin-acetazolamide hybrids that are potent and isoform selective inhibitors of carbonic anhydrases[35]. Hackel et al. displayed a fibronectin protein library on the yeast surface,

with a cysteine coupled to acetazolamide through a maleimide-PEG linker, as showcased in Figure 1.5. Carbonic anhydrases are a family of zinc metalloanzymes that catalyze the interconversion of HCO_3^- and CO_2 and are relevant therapeutic targets due to their involvement in several key biological processes related to HCO_3^-/CO_2 transport or pH control. The hCA isoform used in this work is hCA-II, which has been associated with proliferative diabetic retinopathy, but other isoforms such as hCA-IX, have been related to tumor hypoxia and invasiveness[36]. Engineering isoform specific hybrids is crucial in targeting these issues separately and efficiently, and further understanding what hybrids can bind and/or inhibit carbonic anhydrases will enhance our understanding of these enzymes and their involvement in cancer and other diseases.

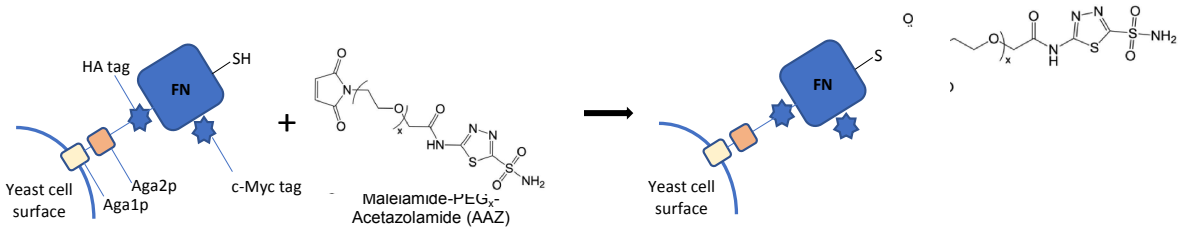


Figure 1.5. Representation of Hackel lab fibronectin-AAZ hybrids. Fibronectins are displayed on the yeast surface, and the cysteine residue reacts with maleiamide-PEG_x-AAZ. The clones had cysteine residues at different positions in the fibronectins, and the PEG linkers were varied in length.

Huang et al.'s work with fibronectins

In Huang's work, six of the fibronectin clones Hackel et al. developed were used (Table 1.1, code names in bold), inserting their sequences into the pCT40 plasmid, and changing the cysteine codon into a TAG codon to allow for amber suppression and the site-specific incorporation of ncAAs of interest[37]. CuAAC was then employed to conjugate sulfonamides onto the fibronectin clones and hybrids were then subjected to binding and inhibition assays with human

carbonic anhydrases II and IX. Huang et al. found that hybrids are more inhibitory than one of the small molecules alone (4-ethynylbenzenesulfonamide), providing a strong case for the construction of protein-small molecule hybrids to enhance warhead inhibitory properties. Hybrids showed binding and inhibitory effects on human carbonic anhydrases II and IX, which is surprising as the clones were selected by the Hackel lab from a sort using PEG linker and AAZ small molecule. In Huang's research, the linker is a ncAA and the small molecules are sulfonamides, less potent than AAZ, but the results show that exploring further linker-warhead combinations on the fibronectins may be useful for uncovering binding and inhibitory hybrids.

Table 1.1. Hackel Lab Fibronectins

hCA-II specific	hCA-IX specific
FnII.28.1-L5-AAZ (K_i = 24 nM) – **FN2.2**	FnIX.28.1-L2-AAZ (K_i = 8.7 nM) – **FN9.1**
FnII.28.1-L7-AAZ (K_i = 4.8 nM) – **FN2.3**	FnIX.28.1-L5-AAZ (K_i = 3.4 nM) – **FN9.5**
FnII.80.1-L7-AAZ (K_i = 80 nM) – **FN2.14**	FnIX.28.1-L7-AAZ (K_i = 48 nM) – **FN9.7**

Thesis work

The objective of this work is to increase the throughput of copper-catalyzed azide-alkyne cycloadditions involving proteins on the yeast surface, which are usually performed in tubes, by developing a novel procedure on plates that does not negatively impact the extent of reaction or its quality. Efforts to increase CuAAC bioconjugate screening throughput have led Wang et al.[38] to the development of an integrated microfluidic device that can perform up to 1024 CuAAC reactions in parallel. While this system has proven useful for CuAAC reactions conjugating two small molecule drugs, it is not feasible to conjugate a small molecule to proteins displayed on a cellular surface such as yeast. In this work, CuAAC bioconjugation on the yeast surface is scaled

up by performing the reaction in 96-well V-bottom plates instead of the traditional protocol performed in 1.7 mL Eppendorf tubes. The new procedure achieved a 10+ fold improvement in experimental throughput when compared to the traditional method.

As a model system for this study, the same approach as in Huang's research was utilized, inserting the sequences of the six of the fibronectin clones from the Hackel Lab into the pCT40 plasmid, and again, switching the cysteine codon into a TAG codon for amber suppression and site-specific incorporation of ncAAs. Small molecules were conjugated with the ncAAs on the fibronectins using CuAAC. The fibronectin TAG sites have been deemed appropriate for bioconjugation by Hackel et al.'s research, which makes them a robust model system for work on CuAAC reactions and protein-small molecule hybrids.

An initial validation of the new CuAAC technique in plates included a comparison of extent of reaction when CuAAC is performed in a plate versus the procedure in tubes. We observed no differences between extent of reaction between the two procedures and proceeded to study cross contamination risk. The results suggest no inherent risk of sample cross over when performing CuAAC on plates. We performed two proof-of-concept studies after ensuring the CuAAC reaction on a plate led to an extent of reaction comparable to that in tubes. The first study is an extensive screening of CuAAC reaction conditions using fibronectin-small molecule conjugates as a model system to further understand how certain parameters, such as yeast cell density, small molecule concentration or temperature, may affect the extent of reaction, which can in turn help future design of experiments by better understanding the reaction landscape. Inspired by the work of Hackel and colleagues, as well as Huang et al., the second line of research involved the evaluation of a combinatorial set comprised of six fibronectins and 27 small molecular drugs to assess extent

of reaction as well as hybrid binding to human carbonic anhydrase. Our screening led to the discovery a new human carbonic anhydrase II binding conjugate.

Overall, performing CuAAC on plates has proved useful to increase experimental scale and screen a wide range of properties and candidates, which will advance the study of protein-small molecule conjugates. Ultimately, this research sets a foundation for future work on the bioconjugation of small molecules to proteins expressed on the yeast surface and sets a precedent for possible automatization of CuAAC reactions to explore the vast combinatorial space of hybrids that could potentially bind and/or inhibit to therapeutic targets of interest.

Chapter 2 details materials and experimental procedures for all reactions and assays performed. In Chapter 3, all results are presented and discussed, and it includes a) a detailed description of the new CuAAC procedure in plates and quality studies, b) the study of CuAAC reaction conditions and c) the screening for potential hCA-II binding protein-small molecule conjugates. Lastly, Chapter 4 elaborates on conclusions from this work and proposes future projects that can be undertaken with this work's findings.

References

1. Lang, K., & Chin, J. W. (2014). Bioorthogonal reactions for labeling proteins. *ACS Chemical Biology*, *9*(1), 16–20.
2. Bird, R. E., Lemmel, S. A., Yu, X., & Zhou, Q. A. (2021). Bioorthogonal chemistry and its applications. *Bioconjugate Chemistry*, *32*(12), 2457–2479.
3. Shih, H.-W., Kamber, D. N., & Prescher, J. A. (2014). Building better bioorthogonal reactions. *Current Opinion in Chemical Biology*, *21*, 103–111.
4. Patterson, D. M., Nazarova, L. A., & Prescher, J. A. (2014). Finding the right (bioorthogonal) chemistry. *ACS Chemical Biology*, *9*(3), 592–605.
5. Presolski, S. I., Hong, V. P., & Finn, M. G. (2011). Copper□catalyzed azide–alkyne click chemistry for Bioconjugation. *Current Protocols in Chemical Biology*, *3*(4), 153–162.
6. Marchand, J. A., Neugebauer, M. E., Ing, M. C., Lin, C.-I., Pelton, J. G., & Chang, M. C. (2019). Discovery of a pathway for terminal-alkyne amino acid biosynthesis. *Nature*, *567*(7748), 420–424.
7. Scinto, S.L., Bilodeau, D.A., Hincapie, R. *et al.* Bioorthogonal chemistry. *Nature Reviews Methods Primers* **1,** 30 (2021).
8. Huisgen, R. (1963). Kinetics and mechanism of 1,3-dipolr cycloadditions. *Angewandte Chemie International Edition in English*, *2*(11), 633–645.
9. Tornøe, C. W., Christensen, C., & Meldal, M. (2002). Peptidotriazoles on solid phase: [1,2,3]-triazoles by regiospecific copper(i)-catalyzed 1,3-dipolar cycloadditions of terminal alkynes to azides. *The Journal of Organic Chemistry*, *67*(9), 3057–3064.

10. Rostovtsev, V. V., Green, L. G., Fokin, V. V., & Sharpless, K. B. (2002). A stepwise Huisgen cycloaddition process: Copper(i)-catalyzed regioselective "ligation" of azides and terminal alkynes. *Angewandte Chemie International Edition*, *41*(14), 2596–2599.
11. Kolb, H. C., & Sharpless, K. B. (2003). The growing impact of Click Chemistry on Drug Discovery. *Drug Discovery Today*, *8*(24), 1128–1137.
12. Hein, J. E., & Fokin, V. V. (2010). Copper-catalyzed azide–alkyne cycloaddition (cuaac) and beyond: New reactivity of copper(i) acetylides. *Chemical Society Reviews*, *39*(4), 1302.
13. Zhu, L., Brassard, C. J., Zhang, X., Guha, P. M., & Clark, R. J. (2016). On the mechanism of copper(i)-catalyzed azide-alkyne cycloaddition. *The Chemical Record*, *16*(3), 1501–1517.
14. Haldón, E., Nicasio, M. C., & Pérez, P. J. (2015). Copper-catalysed azide–alkyne cycloadditions (cuaac): An update. *Organic & Biomolecular Chemistry*, *13*(37), 9528–9550.
15. Yang, M., Jalloh, A. S., Wei, W., Zhao, J., Wu, P., & Chen, P. R. (2014). Biocompatible click chemistry enabled compartment-specific ph measurement inside E. coli. *Nature Communications*, *5*(1).
16. Wu, A. M., & Senter, P. D. (2005). Arming antibodies: Prospects and challenges for immunoconjugates. *Nature Biotechnology*, *23*(9), 1137–1146.
17. Zhao, P., Zhang, Y., Li, W., Jeanty, C., Xiang, G., & Dong, Y. (2020). Recent advances of antibody drug conjugates for clinical applications. *Acta Pharmaceutica Sinica B*, *10*(9), 1589–1600.

18. Diamantis, N., & Banerji, U. (2016). Antibody-drug conjugates—an emerging class of cancer treatment. *British Journal of Cancer*, *114*(4), 362–367.

19. Panowski, S., Bhakta, S., Raab, H., Polakis, P., & Junutula, J. R. (2013). Site-specific antibody drug conjugates for cancer therapy. *MAbs*, *6*(1), 34–45.

20. Nejadmoghaddam, M. R., Minai-Tehrani, A., Ghahremanzadeh, R., Mahmoudi, M., Dinarvand, R., & Zarnani, A. H. (2019). Antibody-Drug Conjugates: Possibilities and Challenges. *Avicenna journal of medical biotechnology*, *11*(1), 3–23.

21. Kang, M., Lu, Y., Chen, S., & Tian, F. (2018). Harnessing the power of an expanded genetic code toward next-generation biopharmaceuticals. *Current Opinion in Chemical Biology*, *46*, 123–129.

22. Xiao, H., & Schultz, P. G. (2016). At the interface of Chemical and biological synthesis: An expanded genetic code. *Cold Spring Harbor Perspectives in Biology*, *8*(9).

23. Xiao, H., Chatterjee, A., Choi, S.-hyun, Bajjuri, K. M., Sinha, S. C., & Schultz, P. G. (2013). Genetic incorporation of multiple unnatural amino acids into proteins in mammalian cells. *Angewandte Chemie International Edition*, *52*(52), 14080–14083.

24. Cellitti, S. E., Jones, D. H., Lagpacan, L., Hao, X., Zhang, Q., Hu, H., Brittain, S. M., Brinker, A., Caldwell, J., Bursulaya, B., Spraggon, G., Brock, A., Ryu, Y., Uno, T., Schultz, P. G., & Geierstanger, B. H. (2008). *in vivo*incorporation of unnatural amino acids to probe structure, dynamics, and ligand binding in a large protein by nuclear magnetic resonance spectroscopy. *Journal of the American Chemical Society*, *130*(29), 9268–9281. https://doi.org/10.1021/ja801602q

25. Liu, C. C., & Schultz, P. G. (2010). Adding new chemistries to the genetic code. *Annual Review of Biochemistry*, *79*(1), 413–444.

26. Johnson, J. A., Lu, Y. Y., Van Deventer, J. A., & Tirrell, D. A. (2010). Residue-specific incorporation of non-canonical amino acids into proteins: Recent developments and applications. *Current Opinion in Chemical Biology*, *14*(6), 774–780.

27. Dabrowski, M., Bukowy-Bieryllo, Z., & Zietkiewicz, E. (2015). Translational Readthrough potential of natural termination codons in eucaryotes – the impact of RNA sequence. *RNA Biology*, *12*(9), 950–958.

28. Chen, H., Venkat, S., McGuire, P., Gan, Q., & Fan, C. (2018). Recent development of genetic code expansion for Posttranslational Modification Studies. *Molecules*, *23*(7), 1662.

29. Chin, J. W. (2017). Expanding and reprogramming the genetic code. *Nature*, *550*(7674), 53–60.

30. Cochran, J., Moore, S., Cochran, F., & Olsen, M. (2009). Cell surface display systems for protein engineering. *Protein Engineering and Design*.

31. Kieke, M. C., Cho, B. K., Boder, E. T., Kranz, D. M., & Wittrup, K. D. (1997). Isolation of anti-T cell receptor scfv mutants by yeast surface display. *Protein Engineering Design and Selection*, *10*(11), 1303–1310.

32. Razai, A., Garcia-Rodriguez, C., Lou, J., Geren, I. N., Forsyth, C. M., Robles, Y., Tsai, R., Smith, T. J., Smith, L. A., Siegel, R. W., Feldhaus, M., & Marks, J. D. (2005). Molecular evolution of antibody affinity for sensitive detection of botulinum neurotoxin type A. *Journal of Molecular Biology*, *351*(1), 158–169.

33. Boder, E. T., & Wittrup, K. D. (1997). Yeast surface display for screening combinatorial polypeptide libraries. *Nature Biotechnology*, *15*(6), 553–557.

34. Van Deventer, J. A., Le, D. N., Zhao, J., Kehoe, H. P., & Kelly, R. L. (2016). A platform for constructing, evaluating, and screening bioconjugates on the yeast surface. *Protein Engineering, Design and Selection*, *29*(11), 485–494.

35. Lewis, A. K., Harthorn, A., Johnson, S. M., Lobb, R. R., & Hackel, B. J. (2022). Engineered protein-small molecule conjugates empower selective enzyme inhibition. *Cell Chemical Biology*, *29*(2).

36. Mocharla, V. P., Colasson, B., Lee, L. V., Röper, S., Sharpless, K. B., Wong, C.-H., & Kolb, H. C. (2004). In situ click chemistry: Enzyme-generated inhibitors of carbonic anhydrase II. *Angewandte Chemie*, *117*(1), 118–122.

37. Huang M., Harthorn, A., Hackel, B. J. & Van Deventer, J. A. Fibronectin-small molecule hybrid inhibitor with clickable noncanonical amino acids. [Manuscript in preparation].

38. Wang, Y., Lin, W.-Y., Liu, K., Lin, R. J., Selke, M., Kolb, H. C., Zhang, N., Zhao, X.-Z., Phelps, M. E., Shen, C. K., Faull, K. F., & Tseng, H.-R. (2009). An integrated microfluidic device for large-scale in situ click chemistry screening. *Lab on a Chip*, *9*(16), 2281.

Chapter 2: Materials and Methods

Media and plate preparation

Preparation of liquid and solid media was performed following the previously described procedures [1]. The strain RJY100 was constructed using standard homologous recombination based on previous protocols[2].

Buffers

1X PBS was prepared by diluting 10X PBS 1:9 in DI water and adjusting the pH to 7.4. Preparation of 10X PBS has been previously described[3]. 1X PBSA was prepared as 1X PBS, adding 0.1% BSA.

DNA cloning and transformation, and TAG codon introduction

Fibronectin sequences from the Hackel lab were cloned into pCT40 plasmids using NheI and BamHI restriction sites, and primers encoding a TAG codon at the cysteine position in the fibronectins were used to introduce the desired mutations. PCR was used to amplify two DNA segments, using either pCT 40-FN_fwd and the TAG codon introduction site forward primer, or pCT 40-FN_rev and the TAG codon introduction site reverse primer. The primers used for this study are included in Table 2.1, with the substitute TAG codons highlighted in red. Gel electrophoresis was performed on the products to extract the DNA fragments with expected insert size. Gibson assemblies were then performed to recombine said DNA fragments with a pCT40 vector digested at the NheI and BamHI restriction sites. The assemblies were transformed into chemical competent *E. coli* DH5αZ1, and plated on ampicillin-containing LB plates, which were

incubated at 37°C overnight. Colonies were picked and grown to saturation in 5 mL of LB liquid media with ampicillin at 37°C for 16 hours. GenCatch plamid DNA Mini-Prep kits were used to isolate plasmid DNA from the cultures, and the cloned plasmids were digested at the NheI and BamHI and subjected to gel electrophoresis to ensure the presence of desired inserts. Sequencing of plasmids was performed by Quintara Biosciences. Table 2.2 showcases the DNA sequence of the fibronectins used in this research. Cysteine codons are highlighted in blue and are switched to a TAG codon that allows incorporation of the desired noncanonical amino acids. NheI and BamHI restriction sites are highlighted in yellow.

Table 2.1. Primers used for cloning (from Manjie Huang's unpublished work[4])

Primer name	**DNA Sequence**
pCT 40-FN_fwd	GGTGGGTCTGGTGGGGGCGGATCTGCTAGCTCCTCCGACTCTCCG
pCT 40-FN_rev	CAAGTCCTCTTCAGAAATAAGCTTTTGTTCGGATCCCTGAGACGGTTTGTCGATTTCGGT
FN2-2TAG_f	TGACTATTTCTTGGGACTATCCTGATTAGGCTATCTATTACCGTATCACCTACGGCGAA
FN2-2TAG_r	AGGTGATACGGTAATAGATAGCCTAATCAGGATAGTCCCAAGAAATAGTCAGAGAGTTCG
FN2-3TAG_f	GACTATTTCTTGGGACGATTCTGCGGCTTAGGCTCTCTATTACCGTATCACCTACGGCG
FN2-3TAG_r	CGCCGTAGGTGATACGGTAATAGAGAGCCTAAGCCGCAGAATCGTCCCAAGAAATAGTC
FN2-14TAG_f	GTGTACGCTGTAACTGATTATGACTAGATTTCAAACCCAATCAGCATCAATTATCGCA
FN2-14TAG_r	AATTGATGCTGATTGGGTTTGAAATCTAGTCATAATCAGTTACAGCGTACACGGTAATGG
FN9-1 TAG_f	TATTTCTTGGGACTATCATCAGAATGGTTAGGCTGTTTCTTACCGTATCACCTACGGCG
FN9-1 TAG_r	TGATACGGTAAGAAACAGCCTAACCATTCTGATGATAGTCCCAAGAAATAGTCAGAGAG
FN9-5 TAG_f	GACTATTTCTTGGGACGATTATCAGAATTAGGCTGTTTCTTACCGTATCACCTACGGCG
FN9-5 TAG_r	GTGATACGGTAAGAAACAGCCTAATTCTGATAATCGTCCCAAGAAATAGTCAGAGAGTTC

FN9-7 TAG_f	ACTATTTCTTGGGACGATTATTTGTTGTAGGTTTTTTCTTACCG TATCACCTACGGCGAA
FN9-7 TAG_r	TGATACGGTAAGAAAAAACCTACAACAAATAATCGTCCCAAG AAATAGTCAGAGAGTTCG

Table 2.2. Fibronectin DNA sequences (from Manjie Huang's unpublished work[4])

Clone Name	Code	DNA sequence
FnII.28.1-L5-AAZ	2.2	GCTAGCTCCTCCGACTCTCCGCGTAACCTGGAGGTTACCAA CGCAACTCCGAACTCTCTGACTATTTCTTGGGACTATCCTGA TTGCGCTATCTATTACCGTATCACCTACGGCGAAACTGGTG GTAACTCCCCGAGCCAGGAATTCACTGTTCCGGGAACTAAT ACTAATGCGACCATCAGCGGTCTGAAACCGGGCCAGGATTA TACCATTACCGTGTACGCTGTAACTGATTATAGCCTTAGTAA TTCAAACCCAATCAGCATCAATTATCGCACCGAAATCGACA AACCGTCTCAGGGATCC
FnII.28.1-L7-AAZ	2.3	GCTAGCTCCTCCGACTCTCCGCGTAACCTGGAGGTTACCAA CGCAACTCCGAACTCTCTGACTATTTCTTGGGACGATTCTGC GGCTTGCGCTCTCTATTACCGTATCACCTACGGCGAAACTG GTGGTAACTCCCCGAGCCAGGAATTCACTGTTCCGGGAACT TCTTATAATGCGACCATCAGCGGTCTGAAACCGGGCCAGGA TTATACCATTACCGTGTACGCTGTAGCTGATTATAGCCTTCA GTATTCAAACCCAATCAGCATCAATTATCGCACCGAAATCG ACAAACCGTCTCAGGGATCC
FnII.80.1-L7-AAZ	2.14	GCTAGCTCCTCCGACTCTCCGCGTAACCTGGAGGTTACCAA CGCAACTCCGAACTCTCTGACTATTTCTTGGGACTATCATTA TCTTGCTCTCTATTACCGTATCACCTACGGCGAAACTGGTGG TAACTCCCCGAGCCAGGAATTCACTGTTCCGGGAAATACTT ATGCGACCATCAGCGGTCTGAAACCGGGCCAGGATTATACC ATTACCGTGTACGCTGTAACTGATTATGACTGCATTTCAAAC CCAATCAGCATCAATTATCGCACCGAAATCGACAAACCGTC TCAGGGATCC
FnIX.28.1-L2-AAZ	9.1	GCTAGCTCCTCCGACTCTCCGCGTAACCTGGAGGTTACCAA CGCAACTCCGAACTCTCTGACTATTTCTTGGGACTATCATCA GAATGGTTGCGCTGTTTCTTACCGTATCACCTACGGCGAAA CTGGTGGTAACTCCCCGAGCCAGGAATTCACTGTTCCGGGT TATTACGATACCTATTCCGCGACCATCAGCGGTCTGAAACC GGGCCAGGATTATACCATTACCGTGTACGCTGTAACCGGTT ATAACGACGATTCAAACCCAATCAGCATCAATTATCGCACC GAAATCGACAAACCGTCTCAGGGATCC
FnIX.28.1-L5-AAZ	9.5	GCTAGCTCCTCCGACTCTCCGCGTAACCTGGAGGTTACCAA CGCAACTCCGAACTCTCTGACTATTTCTTGGGACGATTATCA GAATTGCGCTGTTTCTTACCGTATCACCTACGGCGAAACTG GTGGTAACTCCCCGAGCCAGGAATTCACTGTTCCGGGTTAT

		TACGATACCTATTCCGCGACCATCAGCGGTCTGAAACCGGG CCAGGATTATACCATTACCGTGTACGCTGTAACCGGTTATA ACGACGATTCAAACCCAATCAGCATCAATTATCGCACCGAA ATCGACAAACCGTCTCAGGGATCC
FnIX.28.1-L7-AAZ	9.7	GCTAGCTCCTCCGACTCTCCGCGTAACCTGGAGGTTACCAA CGCAACTCCGAACTCTCTGACTATTTCTTGGGACGATTATTT GTTGTGCGTTTTTTCTTACCGTATCACCTACGGCGAAACTGG TGGTAACTCCCCGAGCCAGGAATTCACTGTTCCGGGATATA CTAATACTGTGACCATCAGCGGTCTGAAACCGGGCCAGGAT TATACCATTACCGTGTACGCTGTAACTACTTATGACCTTGAT TCAAACCCAATCAGCATCAATTATCGCACCGAAATCGACAA ACCGTCTCAGGGATCC

Yeast transformations

Chemically competent RJY100 cells (Ura auxotrophic marker) were transformed with the pCT40 backbone display plasmids showcased in Table 2.3, which contains a Trp auxotrophic marker, and the aaRS/tRNA suppressor plasmid pRS-315 LeuOmeRS for the incorporation of AzMF or OPG, which contains a Leu auxotrophic marker. Transformations were performed following previously described methods[5]. Cells were plated on SD-SCAA (-TRP, -LEU, -URA) solid media and grown for 2-3 days at 30°C.

Noncanonical amino acid preparation

Noncanonical amino acids (ncAAs) were prepared in 50 mM liquid stock by dissolving the ncAA in sterile water volume and vortexing thoroughly. If the ncAA did not fully dissolve, a small volume of 6 N or 1 N NaOH was added. The liquid stock was sterile filtered using a 0.2 µm filter, and was used immediately or stored at 4°C.

Table 2.3. Reporter and suppression plasmid constructs (adapted from Huang's unpublished work[4])

	Backbone	**Auxotrophic marker**	**Clone**	**ncAA**
Display plasmid	pCT40	Trp	FnII.28.1-L5-AAZ	N/A
			FnII.28.1-L7-AAZ	
			FnII.80.1-L7-AAZ	
			FnIX.28.1-L2-AAZ	
			FnIX.28.1-L5-AAZ	
			FnIX.28.1-L7-AAZ	
TAG codon suppression machinery	pRS315	Leu	LeuOmeRS	p-azidomethyl-L-phenylalanine (AzMF) p-propargyloxyphenylalanine (OPG)

Cell culture and induction

Colonies containing the reporter and suppression constructs of interest were inoculated in 5 mL of selective media SD-SCAA (-TRP, -LEU, -URA) and grown to saturation at 30°C in a shaking incubator over 2-3 days. As an alternative, saturated culture samples stored at 4°C were diluted to an OD_{600} value of ~1 by pelleting the cells, aspirating the supernatant, and resuspending in 5 mL of fresh SD-SCAA (-TRP, -LEU, -URA) media. Samples were grown to saturation overnight in a shaking incubator. Once samples were saturated, the cultures were diluted to an OD_{600} of 1 in 5 mL of fresh SD-SCAA (-TRP, -LEU, -URA) media and grown at 30°C in a shaking incubator for 4-8 hours to mid log phase (OD_{600} 2-5). Cells were pelleted and resuspended to an OD_{600} of 1 in 2 mL fresh induction media SG-SCAA (-TRP, -LEU, -URA). Induction media was supplemented with noncanonical amino acids *p*-azidomethyl-L-phenylalanine (AzMF) or *p*-propargyloxyphenylalanine (OPG) to a final concentration of 1 mM.

Copper-catalyzed azide-alkyne cycloaddition click chemistry

Cell Sample Preparation

This procedure is based on the protocol by Hong et al.[6], which was adapted to be performed in plates, changing the reaction volume to 200 μL and the recommended small molecule concentration. OD_{600} values of the cell samples were measured after 16-hour induction at 20°C, and cells were aliquoted in microcentrifuge tubes with 10 million cells each. Tubes were centrifuged at 12,000 rpm for 1 minute at room temperature, the supernatant was aspirated, and the cells were resuspended in 1 mL PBSA (PBS, pH 7.4, 0.1% PBSA) at room temperature. Samples were washed twice more for a total of three PBSA washes. Cells were resuspended in 1 mL PBSA, from which 200 μL aliquots were transferred to specific wells in a 96-well V-bottom plate, yielding 2 million cells per well. For click chemistry performed in tubes, the 200 μL were aliquoted into different tubes. Samples were centrifuged (2 min, 2,400 rpm for plates), and supernatant was decanted (plate samples) or aspirated (tube samples), leaving cells as pellets. For each display construct of interest, two control samples were prepared for click chemistry: a negative control and a DMSO control. The negative control undergoes one-step click chemistry with biotin-$(PEG)_4$-alkyne (AzMF samples) or biotin-$(PEG)_4$-azide (OPG samples, and the DMSO control undergoes two-step click chemistry, first with DMSO and then with biotin-alkyne or biotin-azide. All other samples undergo two-step click chemistry with the small molecule of interest and then with biotin-alkyne or biotin-azide. For two-step click chemistry, cells were used immediately after the washes, whereas for one-step click chemistry, cells were saved as pellets in 4°C. Table 2.4 describes the probes used for each type of experiment and control.

Table 2.4. Reaction Steps & Probes

Experiment	Reaction Step 1 Probe	Reaction Step 2 Probe
Small Molecule Binding – Extent of Reaction Calculations	Small molecule of interest	Biotin-alkyne or biotin-azide
DMSO Control – Extent of Reaction Calculations	DMSO	Biotin-alkyne or biotin-azide
Negative Control – Extent of Reaction Calculations	-	Biotin-alkyne or biotin-azide
Small Molecule Binding – Enzyme Binding Assays	Small molecule of interest	-
DMSO Control – Enzyme Binding Assays	DMSO	-

Reagents

Alkyne-containing small molecules were reconstituted to a final concentration of 100 mM in DMSO, and biotin-$(PEG)_4$-alkyne was reconstituted to 20 mM in DMSO, all stored at -20°C. DMSO was stored in a desiccated jar at room temperature and aliquoted in tubes for each experiment. $CuSO_4$ was reconstituted to 20 mM in sterile water, and THPTA was reconstituted to 50 mM in sterile water, and both were kept at 4°C. $CuSO_4$ and THPTA were mixed in a 1:2 ratio by vortexing in a tube. For the procedure performed on plates, 3 µL of the $CuSO_4$/THPTA mixture were aliquoted in the wells of a 96-well V-bottom plate. Aminoguanadine was reconstituted in sterile water to a concentration of 11 mg/mL and sodium ascorbate was reconstituted in sterile water to a concentration of 20 mg/mL. For the click-chemistry procedure performed on plates, 3 µL of $CuSO_4$ /THPTA mixture were aliquoted in the wells of a 96-well V-bottom plate, and aminoguanidine and sodium ascorbate were transferred to separate wells in a 3-well reservoir to draw required volumes with multi-channel pipettes. For the procedure performed in tubes, all reagents remained in the original tubes in which they were prepared.

Two-step CuAAC on a Plate

The procedure described below details the general reaction conditions used for most experiments in this study. However, conditions of the first reaction, such as small molecule concentration, cell density, reaction time, or temperature, were varied in some cases to study optimal reaction parameters, and this will be described in the results section.

Step 1: Reaction with small molecule of interest. Cell pellets were resuspended in 175 µL 1X PBS at pH 7.4. Then, 2 µL of small molecule (or DMSO for control) were added to each well individually, for a final concentration of 1 mM. Using a multichannel pipette, the 3 µL $CuSO_4$/THPTA aliquots in a separate plate were transferred to each sample, followed by 10 µL of aminoguanadine and 10 µL of sodium ascorbate. Both aminoguanidine and sodium ascorbate reach a final concentration of 5 mM. All steps were performed promptly and pipetting up and down several times after the addition of each reagent to ensure proper mixing. The plate was covered with aluminum foil and left on an orbital shaker at 150 rpm at room temperature for 4 hours. Once the reaction time was over, cells were washed three times with ice-cold PBSA and then left as pellets which could be either used immediately after or saved at 4°C overnight for binding assays with hCA2 or hCA9, or for the second step of the reaction.

Step 2: Reaction with biotin-alkyne probe. Cell pellets were resuspended in 176 µL 1X PBS at pH 7.4. For this step, all reagents are the same except for the small molecule or DMSO, which were substituted by 20 mM biotin alkyne. To each well, 1 µL of biotin-alkyne was added individually. The rest of the procedure is the same as the first step described above, adding 3 µL of $CuSO_4$/THPTA, 10 µL of aminoguanidine and 10 µL of sodium ascorbate in that order. The

plate was covered up with aluminum foil and on left on an orbital shaker at 150 rpm at room temperature for 15 minutes. Once the reaction was over, cells were washed three times in ice-cold PBSA and left as pellets to be prepared for labeling. For negative controls, the first reaction with small molecule or DMSO is omitted, and the cells are only subjected to this reaction with the biotin-alkyne probe. The reagent concentrations and volumes can be found in Table 2.5.

Table 2.5. Click Chemistry Reagents

Compound	Stock Concentration	Volume	Final Concentration	Reaction Step
Small Molecule	100 mM	2 µL	1 mM	Step 1
Biotin-alkyne or Biotin azide	20 mM	1 µL	0.1 mM	Step 2
$CuSO_4$/THPTA	20 mM $CuSO_4$ 50 mM THPTA	3 µL	0.1 mM $CuSO_4$ 0.5 mM THPTA	Steps 1 & 2
Aminoguanadine	11 mg/mL	10 µL	5 mM	Steps 1 & 2
Sodium ascorbate	20 mg/mL	10 µL	5 mM	Steps 1 & 2

Two-step CuAAC in Tubes

The click chemistry procedure in tubes was performed as previously described[5,6], except using a reaction volume of 200 µL instead of 250 µL. The difference with the plate procedure described above is that the reagents are all added individually to one tube at a time, vortexing after the addition of each reagent. After all reagents are added, tubes are left in a tube rack covered with aluminum foil.

Human Carbonic Anhydrase II Binding Assay

Human carbonic anhydrase II (hCA-II, Sino Biological 10478-H08E) was kept in -80°C. The enzymes was reconstituted in sterile water to a concentration of 0.25 g/L. The binding assay was performed with cells that had been subjected to one round of click chemistry with a small

molecule of interest, and 50 nM enzyme in 200 μL PBSA on 96-well V-bottom plates. Cells subjected to a round of click chemistry with DMSO were used as negative controls. Cells were resuspended in the appropriate PBSA volume, and hCA-II was added individually to each well, pipetting up and down after each addition. The plate was left shaking at 150rpm for 1 hour at room temperature. Samples were washed three times in ice-cold PBSA to prepare the cells for flow cytometry labeling.

Flow Cytometry Labeling

Primary Labeling

Samples were labeled for flow cytometry in two steps, and the antibodies used for each step differ based on the type of experiment. For each experiment, three controls with 2 million cells each were prepared: an unlabeled sample, and two single-color controls. For primary labeling, the cells were resuspended in 50 μL PBSA with 1:500 of the antibody label. Table 2.6 details the primary labeling conditions for each experiment:

Table 2.6. Primary Labeling Conditions

Experiment	**Label**	**Time**	**Temperature**	**Location**
Click Chemistry Extent of Reaction	Chicken-anti-c-Myc	30 min	RT	Rotary wheel (tubes) or orbital shaker (plates)
hCA-II Binding Assay	Chicken-anti-c-Myc Mouse anti His 3D5	10 min	4°C	Stationary, on ice
Color Controls	Chicken-anti-c-Myc	30 min	RT	Rotary wheel

Secondary Labeling

The remaining steps were performed on ice. Cells were resuspended in ice-cold PBSA and washed twice. Secondary labeling was performed by adding 50 µL of ice cold PBSA with 1:500 dilution of the fluorescent antibodies. Table 2.7 showcases the conditions for secondary labeling for each experiment:

Table 2.7. Secondary Labeling Conditions

Experiment	**Label**	**Time**	**Temperature**	**Location**
Click Chemistry Extent of Reaction	Goat-anti-chicken AlexaFluor 647; Streptavidin. AlexaFluor 488;	15 min	4°C	Stationary, on ice
hCA-II Binding Assay	Goat-anti-chicken AlexaFluor 647; Goat-anti-mouse AlexaFluor 488;	10 min	4°C	Stationary, on ice
Color Controls	Goat-anti-chicken AlexaFluor 647 or 488	15 min	4°C	Stationary, on ice

Flow cytometry

After secondary labeling, cells were washed twice in ice-cold PBSA and left as pellets. Prior to running the samples in the flow cytometry, pellets were resuspended in 200 µL ice cold PBSA (plates) or 500 µL ice cold PBSA (tubes). Samples were run on Attune NxT flow cytometer, and the data was later analyzed with FlowJo software.

Extent of reaction calculations

FCS files from the flow cytometer were imported to FlowJo and analyzed to extract the median fluorescence intensity (MFI) and coefficient of variation (CV). Using these parameters, the click chemistry extent of reaction was calculated on Microsoft Excel following methods previously described[7].

References

1. Van Deventer, J. A., & Wittrup, K. D. (2014). Yeast surface display for antibody isolation: Library Construction, library screening, and affinity maturation. *Methods in Molecular Biology*, 151–181.
2. Van Deventer, J. A., Kelly, R. L., Rajan, S., Wittrup, K. D., & Sidhu, S. S. (2015). A switchable yeast display/secretion system. *Protein Engineering Design and Selection*, *28*(10), 317–325.
3. *10x PBS*. Cold Spring Harbor Protocols. (1970, January 1). Retrieved June 1, 2021, from http://cshprotocols.cshlp.org/content/2007/4/pdb.rec10768.full?text_only=true
4. Huang M., Harthorn, A., Hackel, B. J. & Van Deventer, J. A. Fibronectin-small molecule hybrid inhibitor with clickable noncanonical amino acids. [Manuscript in preparation].
5. Hershman, R. L., Rezhdo, A., Stieglitz, J. T., & Van Deventer, J. A. (2022). Engineering proteins containing noncanonical amino acids on the yeast surface. *Methods in Molecular Biology*, 491–559.
6. Presolski, S. I., Hong, V. P., & Finn, M. G. (2011). Copper□catalyzed azide–alkyne click chemistry for Bioconjugation. *Current Protocols in Chemical Biology*, *3*(4), 153–162.
7. Stieglitz, J. T., & Van Deventer, J. A. (2022). Incorporating, quantifying, and leveraging noncanonical amino acids in yeast. *Methods in Molecular Biology*, 377–432.

Chapter 3: Results and Discussion

3.1. Assessing the quality of CuAAC performed in plates

Introduction

"Click chemistry" is a concept that was first defined in 2001 by Sharpless et al. to encompass reactions that conjugate molecular entities in a selective and high yield manner, forming stereo- and regioselective products with heteroatom links (C-X-C), under water-tolerant conditions without leading to the formation of byproducts[1]. Copper-catalyzed azide-alkyne cycloadditions (CuAAC) are by far the most popular "click chemistry" reactions, as they are also bioorthogonal, meaning the functional groups involved lack reactivity with surrounding biological entities[2]. CuAAC is known to be compatible with surface display technologies, allowing for bioconjugation on yeast[3,4,5], *E. coli*[6] and mammalian cells[7] for example.

Developing a new protocol in plates

Van Deventer et al. have established the yeast surface as a robust platform for the conjugation and screening of protein-small molecule hybrids using CuAAC, with bioconjugations performed in 1.7 mL Eppendorf tubes[3,4,5]. However, the experimental scale of this procedure is limited from a technical standpoint to 20-30 samples per experiment. This limitation is due to the requirement of adding multiple reagents to each tube with single channel pipettes, and tedious individual washes of the yeast in each tube to terminate the reaction. To increase the scale of CuAAC experiments, we investigated a new procedure in which the reaction is performed in 96-well V-bottom plates instead of in 1.7 mL tubes. The CuAAC procedure in tubes involves adding the reagents in order (Figure 3.1) to one tube at a time, vortexing after the addition of each reagent,

and leaving the tubes stationary at room temperature for the desired reaction time. To end the reaction, each tube is washed individually three times by adding buffer, centrifuging, and aspirating the supernatant. This procedure may be advantageous for smaller scale experiments where only a few conjugates are being tested, especially if the reaction conditions are different in each separate sample. However, it is extremely time consuming when the sample number increases, leading to low experimental throughput. On the other hand, performing CuAAC in a 96-well V-bottom plate allows for testing of 100+ samples in a day and evaluation of a larger set of hybrids: experimental time is alleviated with the use of multichannel pipettes and up to 96 simultaneous washes to terminate reactions in parallel and label samples. In this plate-based procedure, reagents are added in order with a multichannel pipette, pipetting up and down after the addition of each reagent. Following an incubation to allow the reaction to proceed, the reaction is terminated by washing the samples three times. In our initial implementation here, the buffer used for washing is added to up to eight samples at a time with multichannel pipettes. After centrifuging the plate, the supernatant of all samples is discarded simultaneously by decantation.

Figure 3.1 highlights the CuAAC reagents used and the order in which they are added to the yeast cells containing proteins with ncAAs. The new plate-based protocol is fully described in Chapter 2. The first reagent added to the reaction is the probe, which should contain a complementary functional group to react with the azide or alkyne-containing ncAA present in the protein display on the yeast surface. Then a mixture of copper(I) catalyst and copper-chelating ligand is added, followed by an optional additive, in this case aminoguanidine, and then sodium ascorbate which acts as a reducing agent.

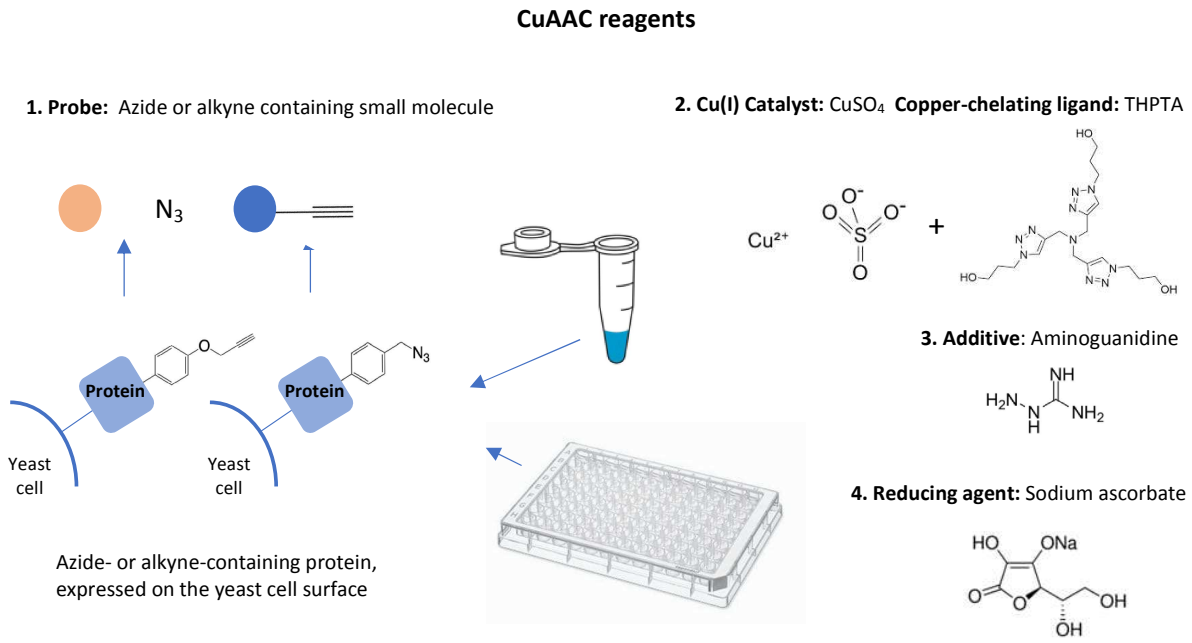


Figure 3.1. Schematic of CuAAC reagents. Cells expressing proteins with azide-containing or alkyne containing ncAAs are placed in a plate or a tube in a reaction buffer, in this case 1X PBS. The first reagent added to the sample is a small molecule probe containing an alkyne or azide group complementary to the functionality present in the displayed protein. Then, a mix of $CuSO_4$ and THPTA is added, followed by aminoguanidine and then sodium ascorbate. Testing in plates allows for up to 96 different small molecule probes to be conjugated to cells, and for the addition of reagents to multiple wells in parallel (here using multichannel pipettes).

Model system: Fibronectins.

A set of six fibronectin clones from the Hackel lab was used as a model system for this work (Tables 1.1 and 2.2). Hackel and coworkers discovered fibronectin-acetazolamide hybrids that can target human carbonic anhydrases II or IX (hCA-II or hCA-IX) selectively and with high affinity[8]. Thiol-maleimide chemistry allowed the conjugation of acetazolamide to an engineered cysteine residue within each fibronectin, but for this work the cysteine codons were replaced by TAG codons (Figure 3.2A) to enable noncanonical amino acid incorporation. The insertion of the ncAA into the protein in response to TAG is ensured by adding both the display construct with the TAG codon, and a suppression construct containing an orthogonal aminoacyl-tRNA

synthetase/tRNA (aaRS/tRNA) pair (Figure3.2B)[9]. Cells were then induced in media supplemented with a ncAA of interest, leading to the site-specific incorporation of the ncAA in the fibronectin structures. The ncAAs used in this study, *p*-azidomethyl-L-phenylalanine (AzMF) and *p*-propargyloxyphenylalanine (OPG), contain bioorthogonal functional groups to facilitate conjugation of small molecules of interest. AzMF has an azide group capable of reacting with alkyne-containing small molecules, and OPG bears an alkyne group capable of reacting with azide-containing small molecules (Figure 3.2C). To quantify extent of reaction, we follow a two-step click chemistry procedure (Figure 3.2D). In the first step, fibronectin-expressing *S. cerevisiae* yeast cells are subjected to CuAAC with a small molecule. In the second step, the cells are reacted with an alkyne-biotin or azide-biotin probe. Cells that successfully undergo CuAAC in the first place will lack sites for biotin conjugation, reducing the amount of biotin present of the cell surface. As a negative control, cells that have not been subjected to a first round of CuAAC are reacted with biotin probes. Then, cells are labeled for the C-terminal affinity tag c-Myc to quantify full protein expression and for biotin to quantify sites not reacted with the small molecule probe of not reacted in the first CuAAC step using flow cytometry analysis. Cells that display full protein expression, and low biotin detection are the ones with higher extent of reaction than those that showcase higer biotin detection.

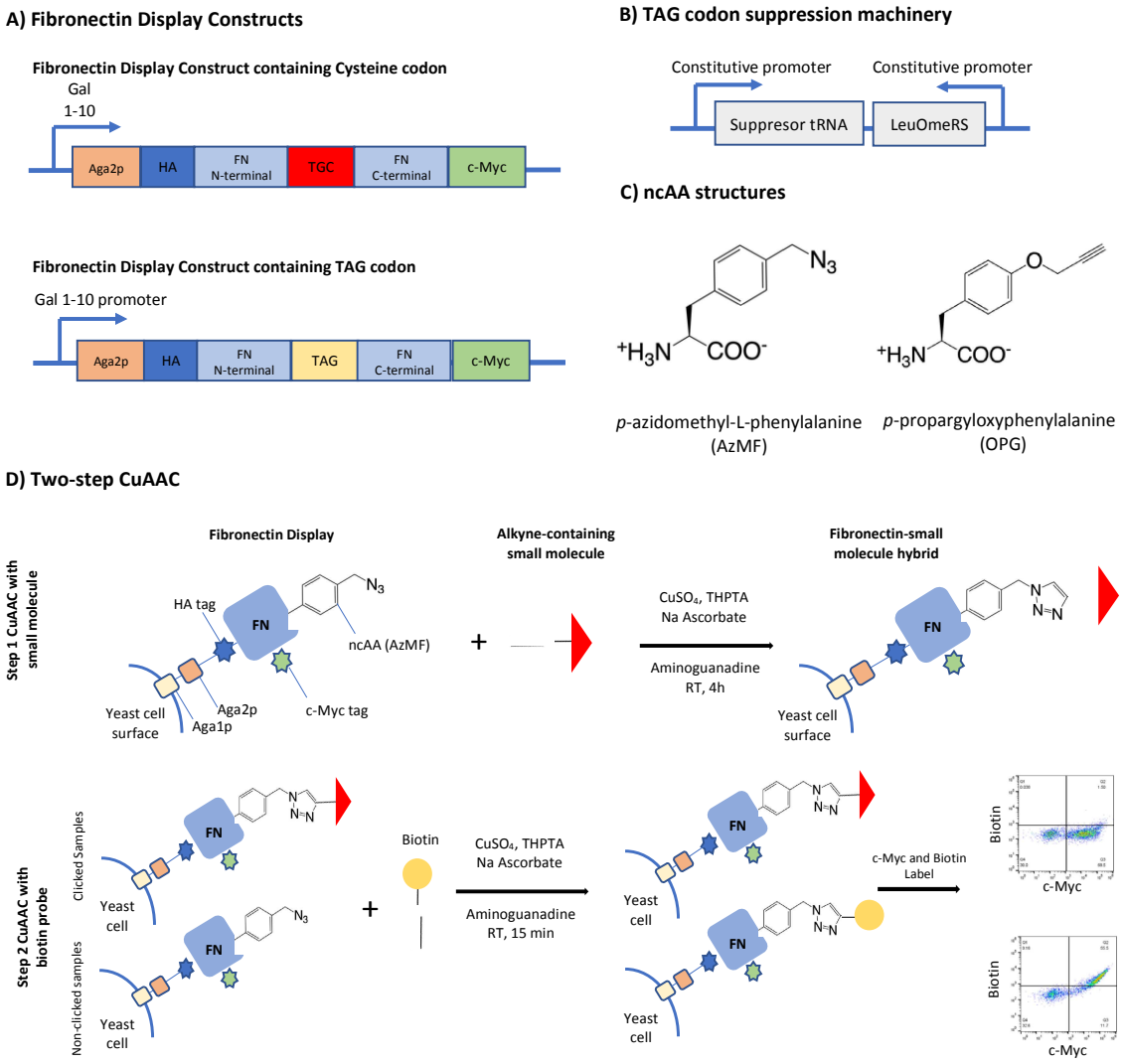


Figure 3.2. Model system diagram. A) Display constructs for fibronectin (FN) expression on the yeast surface. The display construct containing a TGC cysteine codon was developed by the Hackel lab. For this research, the cysteine codon is replaced by a TAG codon for amber suppression. Both constructs encode for yeast surface display anchor Aga2p, HA and c-Myc epitope tags, and the fibronectin clones, with either cysteine or a TAG codon at a position of interest. B) TAG codon suppression constructs combined with display constructs produce full-length proteins after induction in the presence of a ncAA. Orthogonal aaRS/tRNA pairs recognize and incorporate specific sets of ncAAs. In this case, the aminoacyl-tRNA synthetase known as LeuOmeRS incorporates both AzMF and OPG. C) Noncanonical amino acids used in this work: *p*-azidomethyl-L-phenylalanine (AzMF, with azide group that reacts with alkyne-containing molecules), and *p*-propargylozyphenylalanine (OPG, with alkyne group that reacts with azide-containing molecules). D) Diagram of two-step CuAAC procedure to assess extent of reaction. A first reaction with a small molecule of interest is performed under the conditions indicated, followed by a second reaction with a biotin probe that will be conjugated with available ncAA sites on clicked (successful first round) or non-clicked samples (unsuccessful first round or negative control) so that extent of reaction can be measured and quantified using flow cytometry.

Results and Discussion

Quantification of extent of CuAAC reaction in plates compared to tubes

To determine if changing CuAAC reaction procedures affected the extent of reaction, two AzMF-containing fibronectins (FnII.80.1-L7-AAZ and FnIX.28.1-L7-AAZ) were expressed on the surface of yeast and subjected to chemical reactions. Then, CuAAC was performed side-by-side in plates and in tubes in triplicates to conjugate displayed proteins to 4-ethynylbenzenesulfonamide, and to DMSO as a control group, running all samples in triplicates. 4-ethynylbenzenesulfonamide contains an alkyne group that can readily react with AzMF's azide group to form a conjugate. In addition, the aryl sulfonamide warhead present in this molecule is also a known inhibitor of carbonic anhydrase (CA). The sulfonamide functional group present within the molecule can coordinate the enzyme's active site Zn^{2+} ion[10].

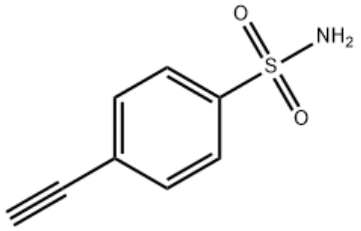


Figure 3.3. Structure of 4-ethynylbenzenesulfonamide. The terminal alkyne group allows for bioconjugation with azide groups through CuAAC, while the benzene ring and sulfonamide functional group interact with the Zn^{2+} active site of carbonic anhydrases, thereby inhibiting these target enzymes.

The extent of reaction of both techniques was calculated using the two-step click chemistry procedure previously described. As a metric to calculate extent of reaction, median biotin detection was used, and only protein-displaying cells (c-Myc positive) were analyzed. Median fluorescence was used instead of mean fluorescence as outlier cells can significantly skew fluorescence values

of flow cytometry samples, making the median fluorescence value preferable for evaluating the data obtained. Flow plots are shown in Figure 3.4A, with the x-axis representing c-Myc detection on each cell, and y-axis illustrating biotin detection, corresponding to available AzMF sites. From the plots, it is clear there are two c-Myc populations (c-Myc positive and c-Myc negative), which is characteristic of the yeast display system used in this work. Qualitative comparison of the flow plots indicates that performing CuAAC in plates results in background levels of biotin detection that are indistinguishable from the level of biotin detection for reactions performed in tubes. Further confirmation is provided by quantitatively evaluating the extent of reaction, represented graphically in Figure 3.4B. Both FnII.80.1-L7-AAZ and FnIX.28.1-L7-AAZ showed an extent of reaction of 96% on plates versus 94% on tubes. Extent of reaction is calculated as detailed in Chapter 2.

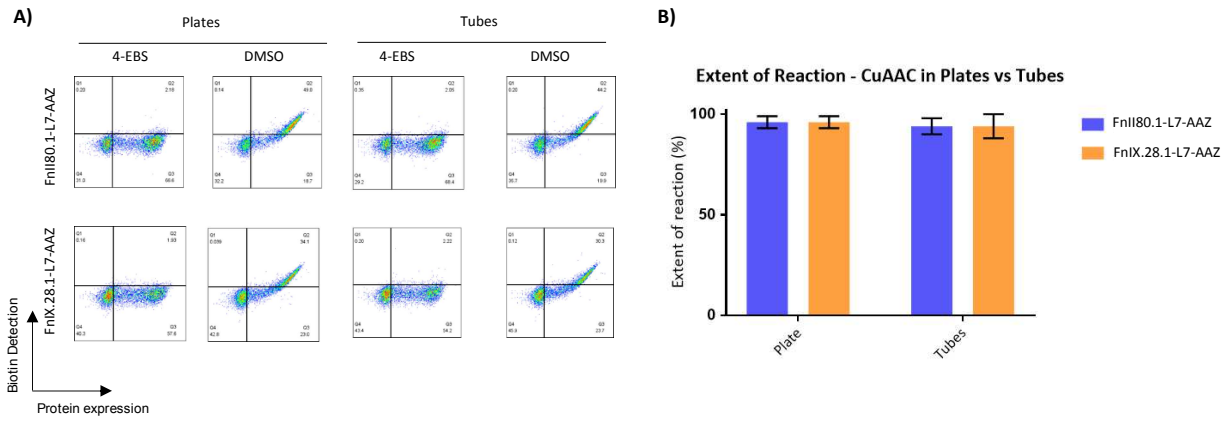


Figure 3.4. Comparison of CuAAC between AzMF and 4-ethynylbenzenesulfonamide in plates versus tubes. A) Representative flow cytometry plots of biotin CuAAC on cells displaying FN2.14 or FN9.7, performed in plates or in tubes as indicated. A first round of CuAAC was performed with 4-ethynylbenzenesulfonamide (4-EBS) or with DMSO as a control. B) Extent of reaction of FnII.80.1-L7-AAZ and FnIX.28.1-L7-AAZ in plates versus tubes. Error bars indicate standard deviation for technical triplicates.

This data illustrates the feasibility of increasing the experimental throughput of CuAAC on the yeast surface as the results are indistinguishable between the procedure perfomed in tubes and the one performed in plates. One of the big differences between performing CuAAC on plates versus tubes, is that in tubes, all reagents are added one-by-one to one tube at a time, but in plates, the first reagent is added to each well, then the second reagent is added to all wells, etc., leading to a timing difference between both methods in between the addition of each reagent. The results show that this difference does not negatively impact the extent of reaction. This experimental set up has the potential to be a robust platform for large scale screening of protein-small molecule hybrids on the yeast surface.

Studying the risk of cross contamination for CuAAC procedure in plates

Once the CuAAC in plates protocol had been established and deemed comparable to the procedure in tubes, the next step was to assess the risk for cross contamination of the new procedure. Because the samples are now set up on a plate, they could be at higher risk of being contaminated by samples in neighboring wells during the procedure due to spillover between wells. To investigate this, again, FnII.80.1-L7-AAZ and FnIX.28.1-L7-AAZ induced in the presence of AzMF were displayed on the yeast surface, but this time the samples were not clicked with a small molecule. Instead, one round of CuAAC was performed with a biotin-alkyne probe or DMSO, and then the cells were labeled for biotin and c-Myc detection. In this case, samples reacted with biotin should show increased fluorescence, and the DMSO reacted samples should not exhibit any fluorescence above background levels unless contaminated. As a control group, the same reactions were also set up in tubes, which should have virtually no risk of cross contamination. The biotin and DMSO samples were set up in plate in two different patterns: 1)

biotin and DMSO samples in separate rows, and 2) biotin and DMSO samples alternating in the plate in a checkerboard pattern (Figure 3.5A). This experiment was performed in technical triplicates. Flow cytometry plots in Figure 3.5B show no fluorescence above background level for samples reacted with DMSO across all three reaction set ups, while samples reacted with biotin exhibit increased fluorescence. This indicates that there is no inherent cross contamination when performing CuAAC in plates, as the DMSO-treated samples do not show any indication of biotin detection.

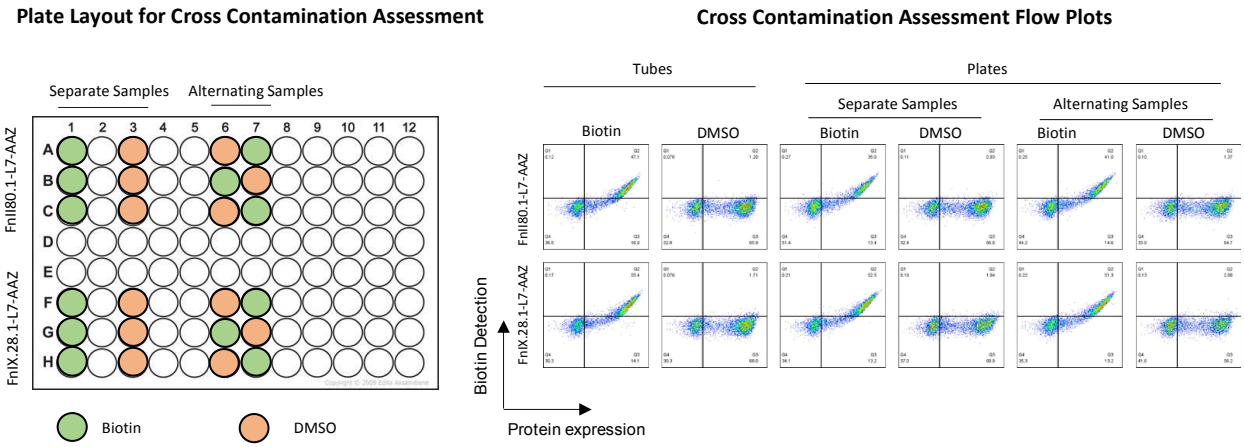


Figure 3.5. Assessment of cross contamination in CuAAC in plates. A) Plate layout for cross contamination assessment experiment. Samples reacted with biotin are represented in green, and samples reacted with DMSO are represented in orange. B) Representative flow plots of biotin CuAAC showcasing the lack of cross contamination when performing CuAAC in plates. .

Conclusion

Sequences for FnII.80.1-L7-AAZ and FnIX.28.1-L7-AAZ containing TAG codons for the incorporation of AzMF were cloned into display vectors and expressed on the yeast surface. The constructs were used to test the efficiency of a CuAAC procedure in plates by comparing the extent of reaction obtained with this technique to that obtained by performing CuAAC in tubes. The

results indicate that increasing the technical scale of the experiment is feasible without affecting reaction quality. We also investigated the potential for cross contamination in plates. No evidence for cross contamination was observed when conducting CuAAC in plates. This suggests that CuAAC can be conducted in plates to generate hybrids with similar quality to those obtained in tubes. Overall, these experiments set the basis for investivating the following: CuAAC reaction conditions and performing a systematic hCA-II binder evaluation campaign.

3.2. Mapping the CuAAC reaction landscape

Introduction

CuAAC is a mechanistically complex reaction, but reliable under a wide range of experimental conditions, such as varying solvents or buffers, additives, and catalysts. Taking advantage of the high-throughput hybrid construction available with the CuAAC procedure in plates, the goal in this work was to further understand conditions that support hybrid construction on the yeast surface. For this work, hybrids were constructed by inducing yeast in the presence of AzMF to display FnII.80.1-L7-AAZ on the yeast surface and using CuAAC on a plate to conjugate different small molecules to FnII.80.1-L7-AAZ and evaluate the extent of reaction across all conditions (a detailed process for extent of reaction calculations is described in Section 3.1). The first set of conditions studied included temperature, small molecule concentration and reaction time across three different small molecules. The small molecules used were 4-ethynylbenzenesulfonamide, pent-4-yne sulfonamide, and 2-(3,4-dihydroxyphenyl)-N-(prop-2-yn-1-yl)acetamide (referred to as catechol-alkyne for simplicity), structures shown in Figure 3.6.



4-ethynylbenzenesulfonamide Pent-4-yne sulfonamide 2-(3,4-dihydroxyphenyl)-N-(prop-2-yn-1-yl)acetamide

Figure 3.6. Structures of small molecules used in first CuAAC reaction conditions study.

As mentioned in the previous section, 4-ethynylbenzenesulfonamide is a known inhibitor of carbonic anhydrases[11]. Pent-4-yne-1-sulfonamide also contains the alkyne group that allows for bioconjugation with AzMF's azide group and contains a sulfonamide group which could potentially interact with the carbonic anhydrase active site. Pent-4-yne-1-sulfonamide is aliphatic so it could show distinct reactivities from the aryl alkyne in 4-ethynylbenzenesulfonamide. Catechol-alkyne was also tested as good extent of reaction has been previously observed with this compound on the yeast surface, and catechol-containing compounds have been found to inhibit human carbonic anhydrase isoenzymes, like hCA IX and XII[12]. We also investigated the effect of incubation conditions (shaking or stationary incubation) was assessed on FnII.80.1-L7-AAZ conjugation with 4-ethynylbenzenesulfonamide. Finally, a study was conducted to understand the effect of yeast cell density and small molecule concentration on the extent of reaction, again using FnII.80.1-L7-AAZ and 4-ethynylbenzenesulfonamide again.

Results and Discussion

Understanding the effect of temperature, small molecule concentration and reaction time on CuAAC extent of reaction

Once the CuAAC protocol on plates was validated, this technique was applied to test out a set of CuAAC reaction parameters to better understand their effects on extent of reaction within the context of the yeast display system. For this set of experiments, FnII.80.1-L7-AAZ induced in the presence of AzMF was used for all conditions. This combinatorial evaluation explored a set of three temperatures (4°C, room temperature and 37°C), three small molecule concentrations (0.1 mM, 0.5 mM, and 1 mM) and four reaction times (1, 2, 3, and 4 hours), performing CuAAC with each of three different small molecules: 4-ethynylbenzenesulfonamide, 10-undecynoic acid and catechol-alkyne. DMSO controls were also obtained for each temperature and time condition. As described in Chapter 2, the extent of reaction is obtained by subtracting the background fluorescence (cell autofluorescence) from the sample MFI and DMSO control MFI, calculating the ratio between the two values, and subtracting it from one. Usually, the background fluorescence is calculated using an unlabeled sample that is not subjected to CuAAC. Initially, the extent of reaction calculations for this work were performed using the unlabeled sample's MFI. However, after visualization of the flow plots, it was clear that using this was not an accurate representation of the extent of reaction, as the MFI for the samples reacted at 37°C (regardless of small molecule) was lower than that of the unlabeled cells. Therefore, for this experiment, the background fluorescence used for each temperature and time condition was the MFI of the c-Myc negative population of the DMSO control. The flow plots obtained for the DMSO controls are depicted in Figure 3.7, demonstrating the lowering of MFI of the c-Myc negative population for samples reacted at 37°C, becoming more apparent as reaction time increases. This could indicate a potential

change in cell or protein behavior at 37°C, which needs to be further studied. While performing CuAAC at 37°C has been reported as beneficial to improve extent of reaction in some cases[13], it should be further studied on yeast because there is a clear change in the y-axis (488 channel) fluorescence that becomes more prominent with increasing incubation time at that temperature. For reference, the DMSO controls used to calculate the for each condition are presented in Figure 3.7.

Figure 3.8 represents the flow cytometry plots obtained for all reaction conditions explored in this study. The lack of fluorescence above background level for most samples means the extent of reaction for most conditions is high, indicating the flexibility of the CuAAC reaction under a wide range of conditions. The shift in MFI for samples reacted at 37°C can also be observed in the samples reacted with small molecules, shown in Figure 3.8 and highlighted in red at the bottom of the page. Samples that show low extent of reaction (4°C, 0.1 mM, 1 hour) are also highlighted. However, the low concentration conditions at 4°C for 2, 3 and 4 hours yield high extent of reaction. We also found that reacting at 37°C led to high extent of reaction one hour so this could be a potential option if shorter reaction times are needed. In Figure 3.9 the extent of reaction is represented quantitatively, showcasing high extent of reactions for most conditions and further confirming our findings from Figure 3.8.

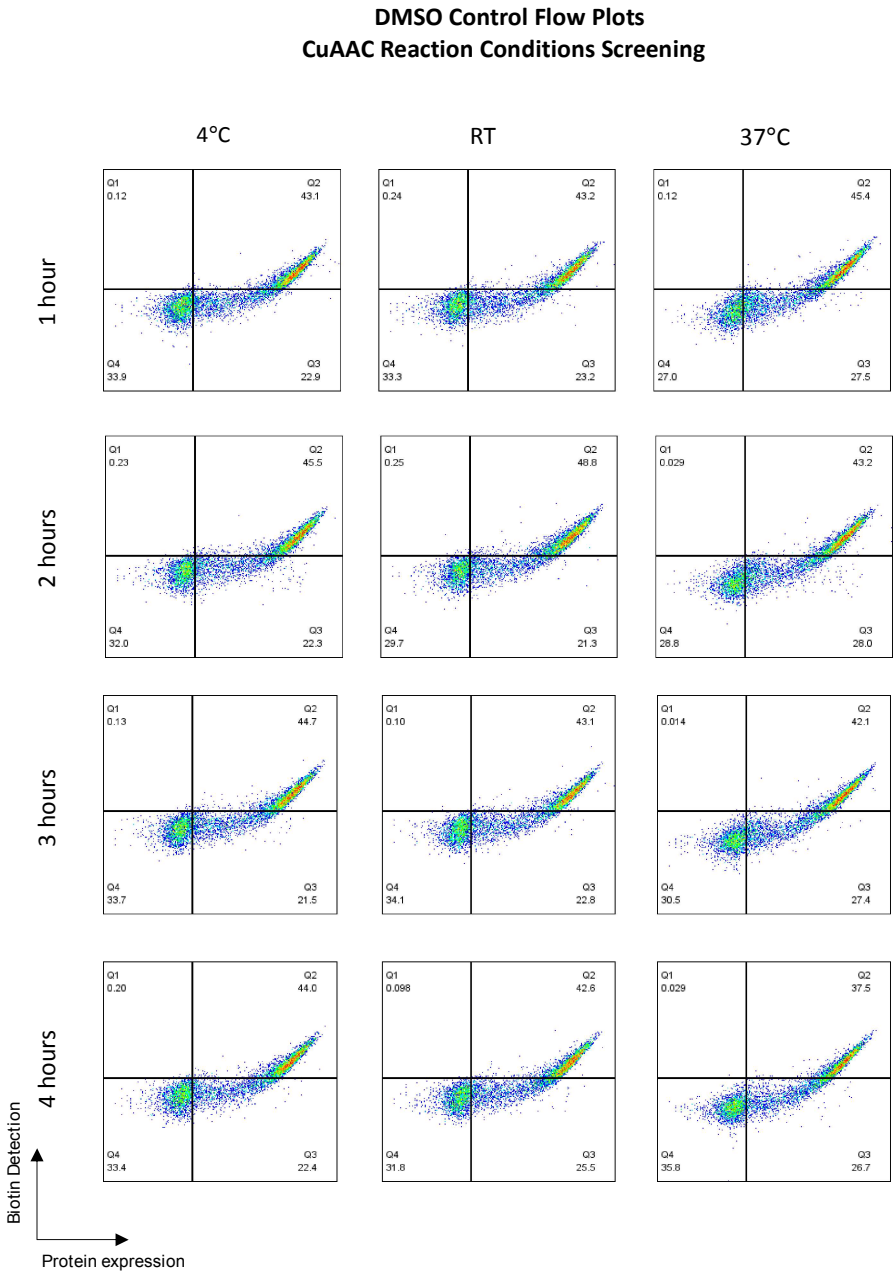


Figure 3.7. Flow plots of DMSO controls for all conditions. The change in fluorescence with 37°C incubation is evident as time increases, making these more accurate than the unlabeled control to calculate the extent of reaction of the other samples.



Figure 3.8. Flow plots of all samples tested for CuAAC reaction parameter evaluation. Highlighted in red are samples discussed in further detail in main writing.

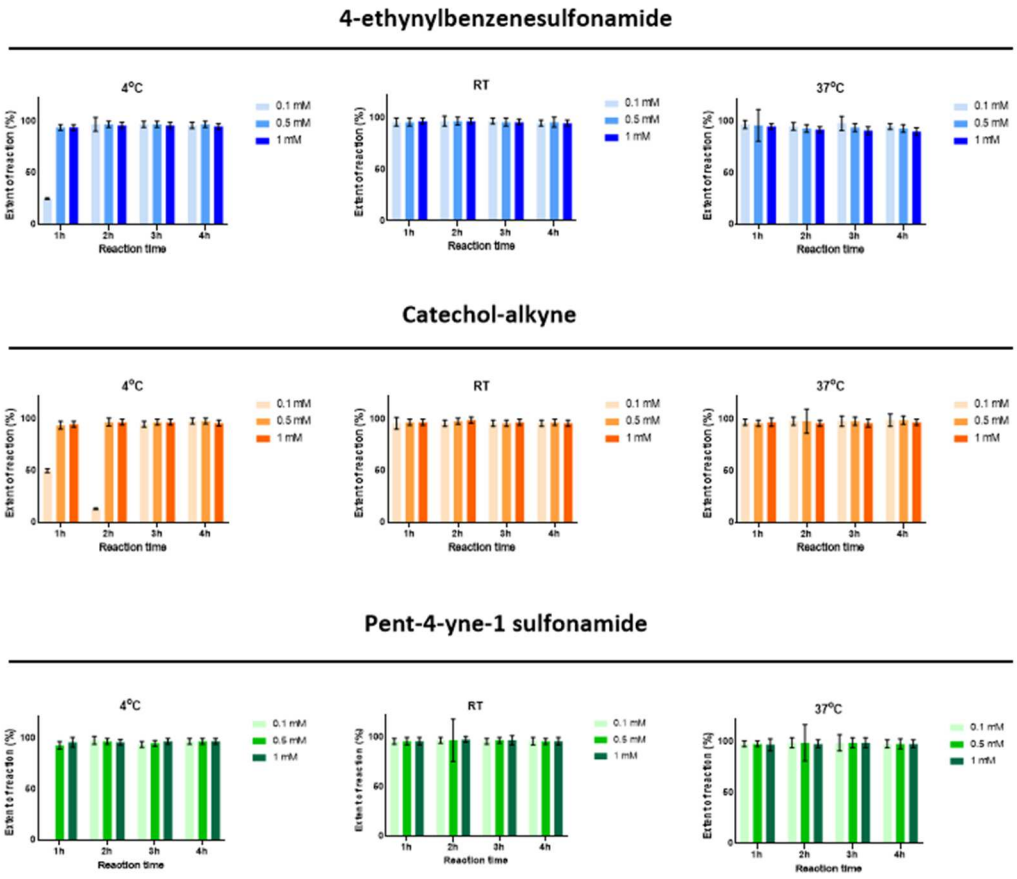


Figure 3.9. Extent of reaction for each condition studied under CuAAC screening. Similarity across conditions reflects flexibility of reaction conditions, except for low temperature and low small molecule concentration conditions.

The high extents of reaction observed in this experiment (above 90% for most conditions) indicate that CuAAC work efficiently across a wide variety of conditions including small molecule concentrations lower than the 1 mM concentration we typically use. Similarity across conditions reflects the flexibility of the reaction and suggest that CuAAC is a permissive reaction, excluding CuAAC with 0.1 mM small molecule at 4°C and for 1 hour.

The results of this study show that performing CuAAC on the yeast surface leads to high extent of reaction conditions under most temperature and time conditions, and under the small molecule concentrations studied. The only condition that led to low extent of reaction was 0.1 mM of small molecules at 4°C and 1 hour, which is an expected finding since reacting with low concentrations of small molecule may need longer reaction time. The temperature could affect some small molecules in a higher degree, for example, reacting 0.1 mM of catechol-alkyne at 4°C had a negative effect on extent of reaction even at 2 hours, which could indicate that this small molecule needs a longer time to react under said conditions. Presolski et al. determined that higher temperatures improved the kinetic of CuAAC reactions by freeing copper ions that could be sequestered by donor groups in surrounding proteins or other biomolecules[5]. This explanation may explain our observations of lowered reaction efficiencies at lower temperatures. Overall, this study demonstrated the wide range of reaction conditions under which CuAAC leads to near-complete reactions on yeast displayed proteins. In following studies, the same conditions described in Chapter 2 (4 hours, room temperature, and 1 mM small molecule) were utilized unless indicated otherwise.

Case study on incubation conditions with 4-ethynylbenzenesulfonamide

For the following studies, the same conditions described in Chapter 2 (4 hours, room temperature, and 1 mM small molecule) were utilized unless indicated otherwise.In the new procedure in plates, samples are incubated on an orbital shaker at 150 rpm to make up for the lack of a vortexing step in between reagent addition. However, this could possibly increase the access of oxygen to the samples. Hong et al.'s protocol[13] recommends capping the reactions to minimize oxygen exposure since it can deplete the reducing agent and lead to an undesired copper(II)-

mediated alkyne-alkyne coupling (Glaser coupling) and the generation of excess reactive oxygen species[13,14]. To understand the if shaking incubation has an effect on the extent of reaction, a study of shaking versus stationary incubation conditions was performed, comparing both methods for the reaction of FnII.80.1-L7-AAZ with 4-ethynylbenzenesulfonamide in technical triplicates. Extents of reaction for each procedure (shaking incubation on a shaking platform versus stationary incubation) are represented in Figure 3.10. The similarity between extents of reaction suggests there is no difference between shaking and stationary samples in the 4-ehtynylbenzenesulfonamide conjugation to FnII.80.1-L7-AAZ (Figure 3.10). This could be because the samples are covered with an aluminum sheet during incubation limiting the access to oxygen. The fact that there is no difference in leaving the samples stationary also suggests that the lack of a vortexing step does not affect reaction extent compared to tubes, and that proper mixing is achieved by pipetting up and down after the addition of each reagent, at least for this reaction. However, further investigation is required to prove this point, as 4-ethynylbenzenesulfonamide conjugates well and leads to very high extent of reaction under all conditions explored. We expect this result to applied when working with well-behaved systems, but additional investigations will shed further light on the extent to which the reaction is oxygen-tolerant over a wide range of conditions, such as small molecules that do not react as well as 4-ethynylbenzenesulfonamide. Another study could be performed with different reaction volumes but equal cell density and stoichiometry in the plate to understand if the excess air space in the well has any effect on extent of reaction. This new high-throughput CuAAC platform for hybrid construction on the yeast surface will help streamline these future investigations.

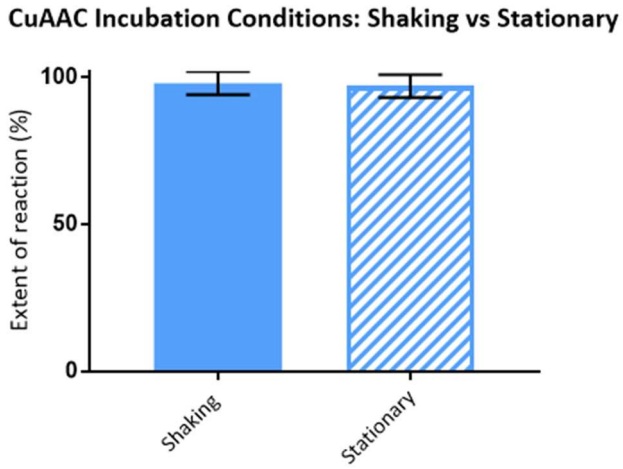


Figure 3.10. Average extent of reaction values from triplicate samples comparing shaking versus stationary incubation conditions. Extent of reaction is not affected by shaking or stationary conditions for this specific conjugation between FnII.80.1-L7-AAZ and 4-ethynylbenzenesulfonamide.

Assessing effect of cell density and small molecule concentration on extent of reaction

Lastly, an assessment of small molecule concentration versus cell density was performed to understand if the cell density can be increased in our experiments or if the small molecule concentrations can be reduced in order to utilize less material. Again, FnII.80.1-L7-AAZ on the yeast surface induced with AzMF was reacted with 4-ethynylbenzenesulfonamides in three concentrations: 0.1 mM, 0.5 mM, and 1 mM. A set of five cell densities was tested, ranging 10, 50, 100, 200 and 400 million cells/mL in the well plates, and the experiment was performed in duplicates. The usual cell density our lab uses for CuAAC is 10 million cells/mL, or 2 million cells per well in a 200 µL reaction. Figure 3.11 shows the extent of reaction for each condition studied. For cell densities below 100 million cells/mL, the extent of reaction does not differ between different small molecule concentrations. However, for samples with cell densities above 100

million cells/mL, the extent of reaction is lowered with decreasing small molecule concentrations. Even though the stoichiometric calculations indicate that small molecules are well in excess, results suggest that the extent of reaction depends on cell density, which could be due to technical limitations when reacting large cell densities in the same well because of mixing difficulty or stoichiometry differences (Figure 3.11). Also, when cell density increases, it seems like higher small molecule concentrations may increase the chance of collision with the proteins and improve the chances of the reaction taking place.

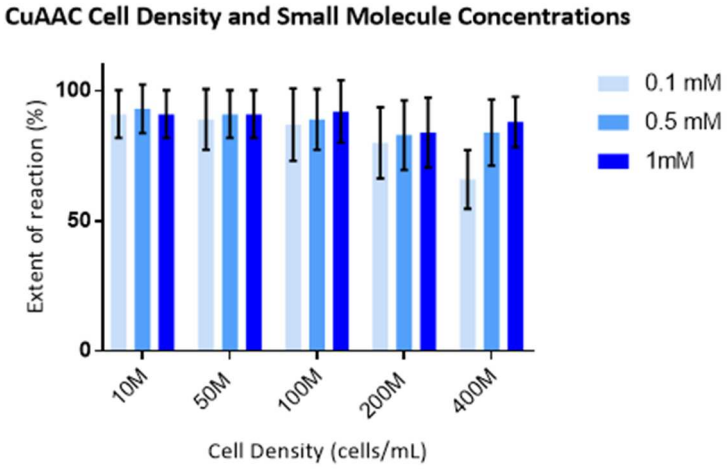


Figure 3.11. Extent of reaction of 4-ethynylbenzenesulfonamide with FnII.80.1-L7-AAZ under different cell density conditions and small molecule concentrations.

Conclusions

A survey of varying reaction times, temperatures, small molecule structures and small molecule concentrations indicated that CuAAC is a flexible and reliable method for the conjugation of azides and alkynes on the yeast surface, with only a few conditions in which the extents of reaction remained low. Lowering of MFI in samples reacted at 37°C was also observed, which could indicate a modification in cell or protein behavior under said conditions and should

be further studied before performing CuAAC at 37°C on the yeast surface. A case study on the effect of shaking incubation on extent of reaction between 4-ethynylbenzenesulfonamide and FnII.80.1-L7-AAZ was performed, which resulted in no obvious differences between shaking and stationary incubation. As mentioned previously, we cannot rule out the possibility that small molecules that do not react as efficiently as 4-ethynylbenzenesulfonamide will follow this trend, so further work could help assess if these systems behave differently under shaking or stationary incubation conditions. Lastly, cell density and small molecule concentration conditions were analyzed, testing the same reaction between 4-ethynylbenzenesulfonamide and FnII.80.1-L7-AAZ using CuAAC. Increasing cell density above 100 million cells/mL negatively impacts the extent of reaction, but higher small molecule concentration can bring the reaction extent back up to completion. These results are also consistent with previous work performed in our tube-based experiments. This could be due to an increase in technical complexity since mixing higher cell densities requires further effort and time pipetting up and down to make sure all cells are resuspended. Overall, this work provided a robust proof-of-concept study for the CuAAC procedure on plates, as it allowed for the testing of a large set of reaction conditions, that would not have been available to analyze as efficiently using a tube-based technique for CuAAC. Our work illuminated some trends and information that can be used in future design of experiments and improve our understanding on CuAAC.

3.3. Human Carbonic Anhydrase II Binding Assay

Introduction

Carbonic anhydrases are enzymes that interconvert carbon dioxide into carbonic acid and bicarbonate ions, and are abundant in mammalian tissues, bacteria, and plants. From a physiological perspective, human carbonic anhydrases convert the carbon dioxide that is diffused out of cells into carbonic acid for it to be carried to the lungs in red blood cells. Once in the lungs, carbonic anhydrases convert the bicarbonate ions back into carbon dioxide prior to exhalation[15]. Carbonic anhydrase affects the regulation of pH, for example, secreting acid in the stomach lining or making saliva neutral. In the eyes, the transport of bicarbonate ions affects the water content in the area, and when the balance is off, there may be a fluid build-up that can cause glaucoma. Inhibiting carbonic anhydrase is a therapeutic strategy to relieve the pressure observed in glaucoma patients. These inhibitors usually bind near the active site, which is a Zn^{2+} ion, blocking its interaction with water and therefore enzymatic action.

Out of all carbonic anhydrase isoforms, human carbonic anhydrase II (hCA-II) is the most widely studied. HCA-II has a central twisted 8-strand beta-sheet surrounded by seven alpha helices, which the zinc ion coordinated by three histidine ligands (His 94, His 96 and His 119) and a water/hydroxyl (Figure 3.12)[16]. The mechanism for reversible hydration of carbon dioxide and bicarbonate can be described in two steps. First the formation of a zinc-bicarbonate complex takes place after the zinc-bound hydroxide attacks the carbon dioxide substrate. Then, the zinc-bound hydroxide is recovered by transferring a proton from the zinc-bound water to the solvent. His 64 may be involved in the intramolecular proton transfer required for this second, changing between two conformations: pointing towards the active side or pointing towards the solvent.

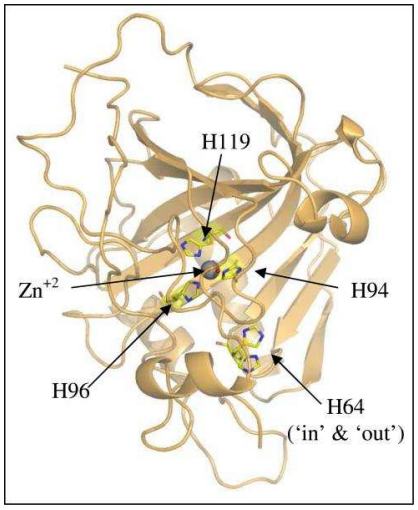


Figure 3.12. Structure of hCA-II. Grey sphere represents zinc atom, and histidine residues are shown in stick model representation. Figure from[16].

In this work, a set of 24 small molecules were conjugated to six different fibronectin clones (FnIX.28.1-L2-AAZ, FnIX.28.1-L5-AAZ, FnIX.28.1-L7-AAZ, FnII.28.1-L5-AAZ, FnII.28.1-L7-AAZ, FnII.80.1-L7-AAZ) on the yeast surface using CuAAC on a plate. The fibronectins were induced with either AzMF (reacted with alkyne-containing small molecules) or OPG (reacted with azide-containing small molecules). Then, half of each sample was transferred to a different plate and subjected to CuAAC with a biotin-alkyne probe (AzMF induced cells) or a biotin-azide probe (OPG induced cells) to assess extent of reaction. The other half were used for a binding assay for 50 nM hCA-II to screen for possible protein-small molecule binders. A compilation of all small molecules is presented in Table 3.1, including the ncAA they react with, and the numerical code used to refer to each compound in the discussion for simplicity. Structural representations of all small molecules are shown in Figure 3.13.

Table 3.1. Small Molecule Information

	Chemical Name	**ncAA**
1	CUDC-101	AzMF
2	10-undecynoic acid	AzMF
3	6-heptynoic acid	AzMF
4	N-hydroxy-10-undecinamide	AzMF
5	2-(3,4-dihydroxyphenyl)-N-(prop-2-yn-1-yl)acetamide	AzMF
6	4-Ethynylbenzene-1-sulfonamide	AzMF
7	Pent-4-yne-sulfonamide	AzMF
8	N-(5-sulfamoyl-1,3,4-thiadiazol-2-yl)hex-5-ynamide	AzMF
9	4-azidobenzenesulfonamide	OPG
10	2-(2-Propyn-1-yloxy)ethanesulfonyl fluoride	AzMF
11	But-3-yne-1-sulfonyl fluoride	AzMF
12	4-ethynylbenzene-1-sulfonyl fluoride	AzMF
13	N-(hept-6-yn-1-yl)-2,3-dihydroxybenzamide	AzMF
14	N-[2-(3,4-dihydroxyphenyl)ethyl]hept-6-ynamide	AzMF
15	3-(but-3-yn-1-yl)-1-[2-(3,4-dihydroxyphenyl)ethyl]thiourea	AzMF
16	N-(2-azidoethyl)-[2,2'-bipyridine]-5-carboxamide	OPG
17	4-azido-N-({[2,2'-bipyridine]-6-yl}methyl)butanamide	OPG
18	N-(5-azidopentyl)-[2,2'-bipyridine]-5-carboxamide	OPG
19	N-(5-azidopentyl)-2-(pyridin-2-yl)quinoline-4-carboxamide	OPG
20	2,3-diamino-5-bromo-N-(hept-6-yn-1-yl)benzamide	AzMF
21	2-propynylurea	AzMF
22	1-phenyl-3-prop-2-yn-1-ylurea	AzMF
23	4-(Dihydroxyborophenyl)acetylene	AzMF
24	4-(propargylaminocarbonyl)phenylboronic acid	AzMF

The set of small molecules is comprised of chemicals purchased by the lab for the inhibition of enzymes such as matrix metalloproteinases, serine hydrolases or human carbonic anhydrases II and IX, mainly by interaction with zinc-ion functional groups. All small molecules contained either

an alkyne or azide functional group to react with one of the ncAAs presented within the fibronectin structures, and a functional group that could potentially bind or inhibit enzymatic active sites. Hydroxamates and carboxylates are non-specific inhibitors of MMPs, which contain a zinc-ion-chelating active site. Because of this, they could also potentially bind to and inhibit the zinc in the active site in carbonic anhydrases. Hydroxamates CUDC-101 (**1**) and N-hydroxy-10-undecinamide (**4**), and carboxylates 10-undecynoic acid (**2**) and 6-heptynoic acid (**3**) were tested in this screening campaign to assess any possible interactions with hCA-II's active site[17]. The catechol-alkyne small molecule (2-(3,4-dihydroxyphenyl)-N-(prop-2-yn-1-yl)acetamide) (**5**) used in the CuAAC reaction conditions study was also analyzed for binding to hCA-II, as some catechol groups have been previously reported to inhibit this CA isoform[18]. A set of sulfonamides were also analyzed, including 4-ethynylbenzenesulfonamide (**6**), pent-4-yne-1 sulfonamide (**7**), N-(5-sulfamoyl-1,3,4-thiadiazol-2-yl)hex-5-ynamide (acetazolamide or AAZ, **8**) and 4-azidobenzenesulfonamide (**9**). Sulfonamides are known inhibitors of hCA-II, fibronectin-sulfonamide compounds have already been assayed with both hCA-II and hCA-IX in unpublished work by Huang et al., showcasing different levels of binding and inhibition[19]. Compound **8**, AAZ, has been previously conjugated through different length PEG linkers to fibronectins expressed on the yeast surface by Hackel et al. and reported to inhibit and bind to hCA as well[20]. Three sulfonyl-fluorides, two aliphatic (**10**,**11**) and one aromatic (**12**), were analyzed as well since sulfonyl fluorides have been previously developed for enzymatic inhibition of serine proteases[21]. Compounds **13-20** had been previously purchased to analyze with MMP9 and include miscellaneous groups such as bipyridine groups or benzamides, which could also potentially interact with the hCA-II active site, as they can form metal complexes, possibly binding to the zinc

in hCA-II. Compounds **21** and **22** contain urea groups, and compounds **23** and **24** are boronates that might interact with hCA-II's zinc atom as well.

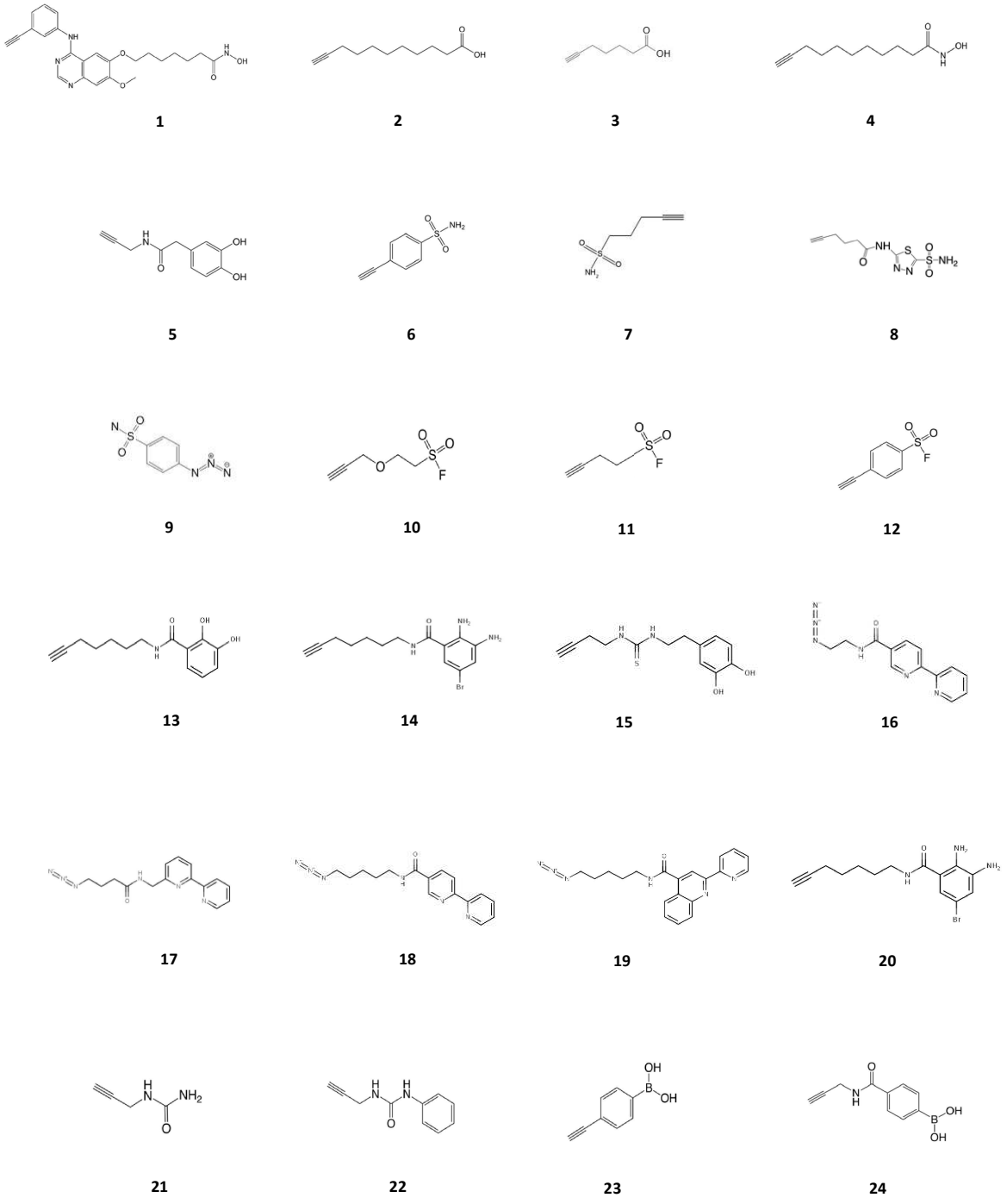


Figure 3.13. Structures of small molecules used in this study. Numbers correspond to the ones indicated for each small molecule in Table 5.1.

Results and Discussion

Extent of Reaction Screening

To identify hCA-II binding protein-small molecule conjugates, the 24 small molecules presented in Table 3.1 and Figure 3.13 were conjugated with all six fibronectins using CuAAC yielding a total of 144 conjugates. The same reaction conditions described in Chapter 2 are used for all small molecules, except for samples reacted with compound **8**, AAZ, which were reacted with 0.1 mM AAZ for 15 minutes because clones lose binding ability if higher concentrations or longer times are used[5]. After CuAAC, half of the sample volume was transferred to a different plate for a second round of CuAAC with a biotin probe, and the remaining sample was incubated with hCA-II for a binding assay.

All hybrids were subject to a second round of CuAAC with a biotin probe to quantify extent of reaction, providing a small molecule reactivity profile. The calculations were performed by subtracting the background MFI of the unlabeled cells the c-Myc positive MFI of each sample. The extent of reaction calculations are described in detail in Chapter 2. Figure 3.16 illustrates the extent of reaction of all small molecules with each fibronectin. This format allows for the rapid visualization of compounds that do not "click" as well as the rest, for example, compounds **4** (N-hydroxy-10-undecinamide), **8** (AAZ, N-(5-sulfamoyl-1,3,4-thiadiazol-2-yl)hex-5-ynamide), **17** (4-azido-N-({[2,2'-bipyridine]-6-yl}methyl)butanamide), show low extent of reaction with all fibronectins. The differences in small molecule reactivity could stem from the small molecule structure and size affecting the access to ncAAs and possibly some unwanted reactivity with cells, disrupting the proteins as it is observed in the case of AAZ. This data once again proves the utility of performing the CuAAC reaction in plates, as the results can serve to rapidly assess which small molecules may be more suited to perform CuAAC with.

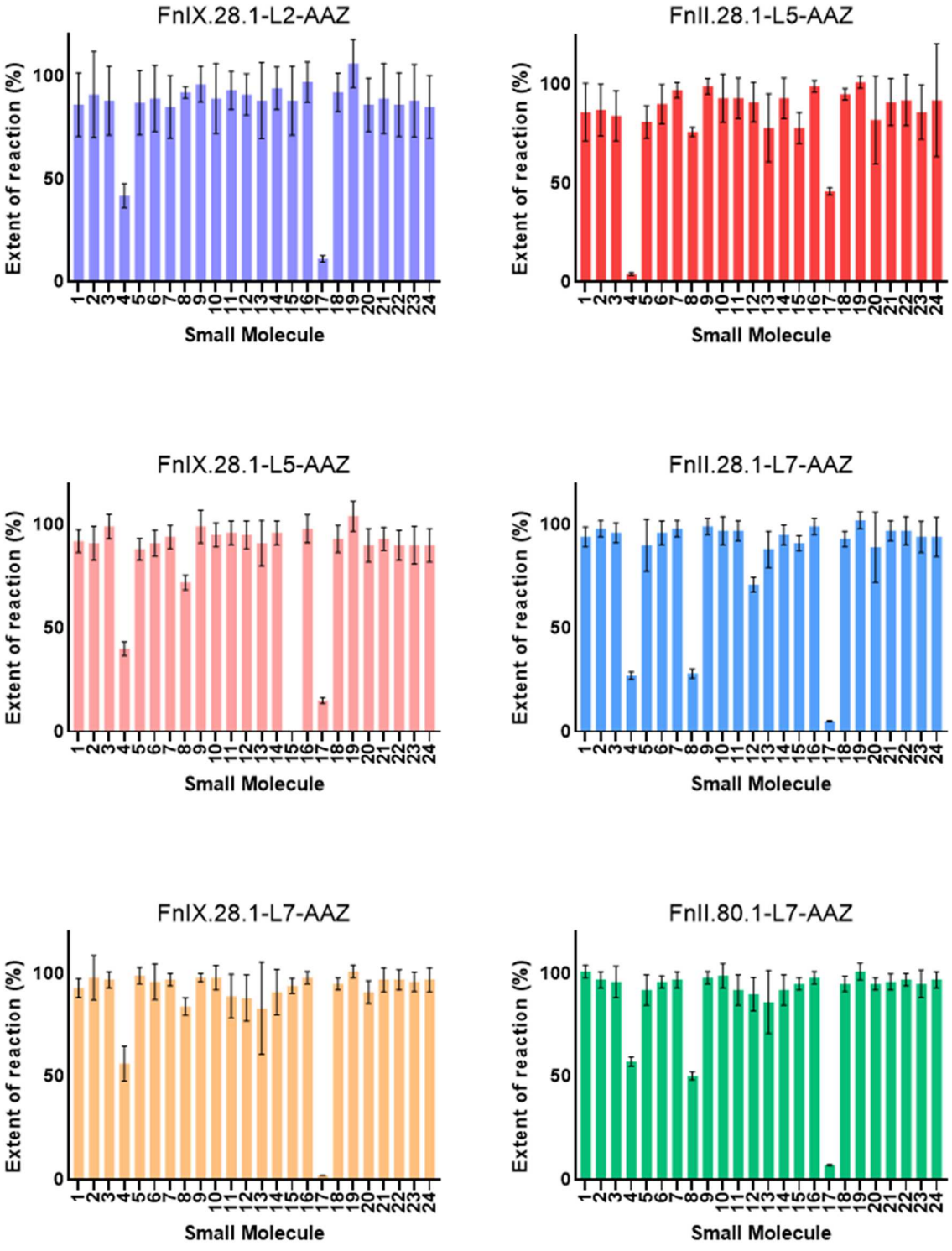


Figure 3.16. Extent of reaction of CuAAC between small molecules and fibronectins. No extent of reaction data is reported for Compound 15 and FnIX.28.1-L5-AAZ due to a technical error that occurred during flow cytometer data recovery.

hCA-II Binding Assay

For the binding assay, the samples were incubated with hCA-II and then labeled for hCA-II and c-Myc detection. The samples that show binding to hCA-II show fluorescence in the y-axis, and again, full protein expression is denoted by fluorescence in the x-axis (Figure 3.14).

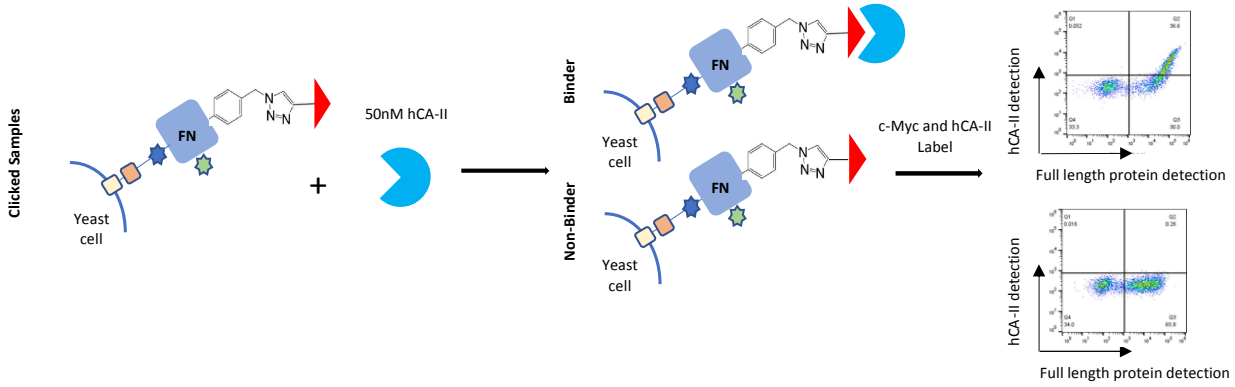


Figure 3.14. Schematic of hCA-II binding assay. Samples are incubated with 50 nM hCA-II and then labeled for c-Myc and hCA-II to be analyzed with flow cytometry. Binders will show both hCA-II and c-Myc detection, and non-binders will not showcase hCA-II detection but will have c-Myc detection.

To compile the hCA-II binding data in a format easy to visualize, the background median fluorescence intensity (MFI) values (c-Myc negative population of DMSO controls) was subtracted from the MFI of the c-Myc positive population of hybrid samples, and the values are represented on the heatmap on Figure 3.15. Higher MFI, which is correlated to binding to hCA-II, is denoted in the heatmap with a stronger shade of blue, which is observed for three samples. The screening led to the confirmation of FnIX.28.1-L7-AAZ-AAZ and FnII.80.1-L7-AAZ-AAZ's binding ability to hCA-II, and the discovery of a functional hybrid: FnIX.28.1-L7-AAZ-4-ethynylbenzenesulfonamide (EBS) (row 6, Figure 3.15).

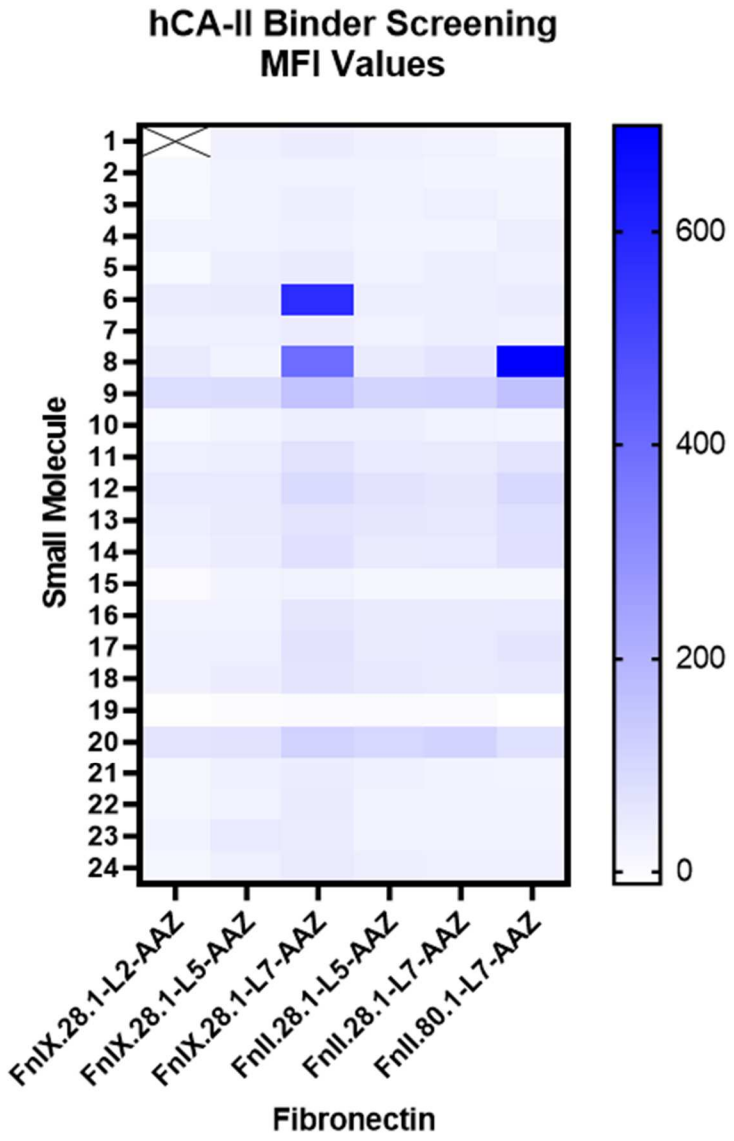


Figure 3.15. hCA-II Binder Screening Results. A) Heatmap of MFI Values for all hybrids screened. Compound 1 and FnIX.28.1-L2-AAZ data is not presented due to technical error with flow plots. The MFI unit is arbitrary, calculated as the background MFI subtracted from c-Myc positive population MFI of each sample. A stronger tone of blue denotes more binding of the hybrid to hCA-II.

4-ethynylbenzenesulfonamide is a known inhibitor of hCA-II, interacting with the enzyme's active site. However, FnIX.28.1-L7-AAZ was sorted as hCA-IX specific by the Hackel

Lab, so it seems like changing the linker and small molecule may change binding properties of the hybrid. This screening served as proof of the utility of performing CuAAC on plates, as a wide range of protein-small molecule hybrids were analyzed with ease and uniformity of conditions, leading to the discovery of a binding hybrid.

Conclusions

The reactivities of different small molecules with fibronectin clones using CuAAC and their binding to human carbonic anhydrase II were analyzed to demonstrate the robustness of performing CuAAC on plates to produce protein-small molecule hybrids. Both the hybrid extent of conjugation and the binding ability to hCA-II were assessed through flow cytometry assays. All six fibronectin clones obtained from the Hackel Lab were conjugated to a set of 24 small molecule with varying functional groups that could potentially show binding or interact with hCA-II's Zn^{2+} active site. Screening the fibronectin-small molecule hybrid space in a high throughput manner can help find hit compounds for enzyme binding or inhibition in less time and find the right combination of warheads and protein binding sites. This study led to the discovery of a new hCA-II binding hybrid, FnIX.28.1-L7-AAZ and 4-ethynylbenzenesulfonamide, and the confirmation of binding of two other fibronectin hybrids (FnIX.28.1-L7-AAZ and FnII.80.1-L7-AAZ) with AAZ (compound **8**).

The extent of reaction of all hybrids was quantified, and trends in small molecule reactivity could be observed easily on plots. Most small molecules can react readily with the ncAA-containing fibronectins, but a few of them showed consistently low reactivities, such as small molecules **4**, **8** and **17**. Small molecule reactivity can also vary between fibronectin clones,

however variations across this factor were less than across small molecule type. These discerned trends between small molecules may be difficult to predict, but further analysis can shed a light on what factors may cause differences in reactivity. Understanding this will help us construct protein-small molecule hybrids in high yield and harness the utility of these compounds to target therapeutically relevant enzymes.

References

1. Kolb, H. C., Finn, M. G., & Sharpless, K. B. (2001). Click chemistry: Diverse chemical function from a few good reactions. *Angewandte Chemie International Edition*, *40*(11), 2004–2021.
2. Lang, K., & Chin, J. W. (2014). Bioorthogonal reactions for labeling proteins. *ACS Chemical Biology*, *9*(1), 16–20.
3. Van Deventer, J. A., Le, D. N., Zhao, J., Kehoe, H. P., & Kelly, R. L. (2016). A platform for constructing, evaluating, and screening bioconjugates on the yeast surface. *Protein Engineering, Design and Selection*, *29*(11), 485–494.
4. Stieglitz, J. T., Potts, K. A., & Van Deventer, J. A. (2021). Broadening the toolkit for quantitatively evaluating noncanonical amino acid incorporation in yeast.
5. Islam, M., Kehoe, H. P., Lissoos, J. B., Huang, M., Ghadban, C. E., Berumen Sánchez, G., Lane, H. Z., & Van Deventer, J. A. (2021). Chemical diversification of simple synthetic antibodies. *ACS Chemical Biology*, *16*(2), 344–359.
6. Yang, M., Jalloh, A. S., Wei, W., Zhao, J., Wu, P., & Chen, P. R. (2014). Biocompatible click chemistry enabled compartment-specific ph measurement inside E. coli. *Nature Communications*, *5*(1).
7. Gutmann, M., Memmel, E., Braun, A. C., Seibel, J., Meinel, L., & Lühmann, T. (2016). Biocompatible azide-alkyne “click” reactions for surface decoration of Glyco-engineered cells. *ChemBioChem*, *17*(9), 866–875.
8. Lewis, A. K., Harthorn, A., Johnson, S. M., Lobb, R. R., & Hackel, B. J. (2022). Engineered protein-small molecule conjugates empower selective enzyme inhibition. *Cell Chemical Biology*, *29*(2).

9. Stieglitz, J. T., Kehoe, H. P., Lei, M., & Van Deventer, J. A. (2018). A robust and quantitative reporter system to evaluate noncanonical amino acid incorporation in yeast. *ACS Synthetic Biology*, *7*(9), 2256–2269.
10. Kacprzak, K. M., Skiera, I., & Rutkowski, J. (2022). 2.5 cuaac and metal-free 1,3-Dipolar Huisgen cycloadditions in drug discovery. *Click Chemistry*.
11. Kacprzak, K. M., Skiera, I., & Rutkowski, J. (2022). 2.5 cuaac and metal-free 1,3-Dipolar Huisgen cycloadditions in drug discovery. *Click Chemistry*.
12. Scozzafava, A., Passaponti, M., Supuran, C. T., & Gülçin, İ. (2014). Carbonic anhydrase inhibitors: Guaiacol and catechol derivatives effectively inhibit certain human carbonic anhydrase isoenzymes (HCA I, II, IX and XII). *Journal of Enzyme Inhibition and Medicinal Chemistry*, *30*(4), 586–591.
13. Presolski, S. I., Hong, V. P., & Finn, M. G. (2011). Copper□catalyzed azide–alkyne click chemistry for Bioconjugation. *Current Protocols in Chemical Biology*, *3*(4), 153–162.
14. Presolski, S. I., Hong, V., Cho, S.-H., & Finn, M. G. (2010). Tailored ligand acceleration of the Cu-catalyzed azide−alkyne cycloaddition reaction: Practical and mechanistic implications. *Journal of the American Chemical Society*, *132*(41), 14570–14576.
15. *PDB101: Molecule of the month: Carbonic anhydrase*. RCSB. (n.d.). Retrieved July 1, 2022, from https://pdb101.rcsb.org/motm/49
16. Avvaru, B. S., Busby, S. A., Chalmers, M. J., Griffin, P. R., Venkatakrishnan, B., Agbandje-McKenna, M., Silverman, D. N., & McKenna, R. (2009). Apo-Human carbonic anhydrase II revisited: Implications of the loss of a metal in protein structure, stability, and Solvent Network. *Biochemistry*, *48*(31), 7365–7372.

17. Hu, J., Van den Steen, P. E., Sang, Q.-X. A., & Opdenakker, G. (2007). Matrix metalloproteinase inhibitors as therapy for inflammatory and vascular diseases. *Nature Reviews Drug Discovery*, *6*(6), 480–498. https://doi.org/10.1038/nrd2308

18. Scozzafava, A., Passaponti, M., Supuran, C. T., & Gülçin, İ. (2014). Carbonic anhydrase inhibitors: Guaiacol and catechol derivatives effectively inhibit certain human carbonic anhydrase isoenzymes (HCA I, II, IX and XII). *Journal of Enzyme Inhibition and Medicinal Chemistry*, *30*(4), 586–591.

19. Huang M., Harthorn, A., Hackel, B. J. & Van Deventer, J. A. Fibronectin-small molecule hybrid inhibitor with clickable noncanonical amino acids. [Manuscript in preparation].

20. Lewis, A. K., Harthorn, A., Johnson, S. M., Lobb, R. R., & Hackel, B. J. (2022). Engineered protein-small molecule conjugates empower selective enzyme inhibition. *Cell Chemical Biology*, *29*(2).

21. Narayanan, A., & Jones, L. H. (2015). Sulfonyl fluorides as privileged warheads in chemical biology. *Chemical Science*, *6*(5), 2650–2659.

Chapter 4: Conclusions and future work

The results obtained in this work provide evidence that performing CuAAC in a high-throughput manner with plate-based method leads to the construction of high-quality protein-small molecule hybrids. Fibronectin proteins were cloned into a display construct containing a TAG codon for amber suppression, and expressed on the yeast surface, inducing with noncanonical amino acids containing functional groups for bioconjugation. Comparing CuAAC performed in plates to our tradition tube-based method revealed that both strategies result in similar extents of reaction and no sample carryover.

Based on these findings, we performed two proof-of-concept studies for surveying reaction conditions and enzyme binding assays that proved the utility of our plate-based approach. The first study analyzed a large set of CuAAC conditions, including reaction temperature, time, small molecule concentration, or cell density. Overall, across all conditions tested, the CuAAC reaction is very permissive, allowing a wide range of temperatures, times, and small molecule concentrations without them having an impact on extent of reaction. A case study was performed to understand the effect of shaking versus stationary incubation conditions for CuAAC, which showed that incubation conditions have no effect on the extent of reaction in a well-behaved system but further studies are required with small molecules that may be more affected by the difference in incubation to determine oxygen sensitivity of the reaction. An analysis of cell density and small molecule concentration led to the conclusion that higher cell densities may benefit from using higher small molecule concentrations, and this may be because of technical difficulties that come with working with such a high cell density in the same well. Overall, our plate-based assays allow for the exploration of the CuAAC reaction space, and permits future testing of other reaction

parameters, such as reagent concentrations, order of addition and possibility of mixing reagents before addition, etc.

Lastly, an evaluation of extent of reaction of a set of 144 protein-small molecule hybrids showcased reactivity profiles of all small molecules, which could be further studied in the future to understand the underlying causes of these differences in extent of reaction. The hybrids were also subjected to an hCA-II binding assay, looking for potential hCA-II binders. This assay led to the discovery of a new FnIX.28.1-L7-AAZ-4-ethynylbenzenesulfonamide binder. This study demonstrates the utility of performing CuAAC in plates as it allows for the analysis of large set of hybrids in a shorter time than when performed in tubes.

Analysis of CuAAC reaction conditions can help improve design of experiments, and the new CuAAC procedure on plates allows for extensive study of parameters that may affect reaction quality. This technique could be used to expand the understanding on biorthogonal reactions on the yeast surface by testing different reagent concentration combinations, or different ligands, or further understanding the effect of incubation conditions such as shaking. CuAAC on plates is also a robust method to screen large numbers of hybrids on the yeast surface and their activity with specific enzymes. Overall, this system has proved useful and effective in increasing the throughput of CuAAC on the yeast surface and sets a precedent for possible automation of lab procedures to construct and evaluate even larger sets of protein-small molecule hybrids. Automation could lead to even more homogeneous experiments, analyzing a large combinatorial space of hybrids in a short time and improving the knowledge on these constructs and their effects on other molecules of therapeutic interest. Being able to test a large collections of hybrids constructed via CuAAC

would greatly enhance the chances of finding binding hybrids, not only to hCA-II, but also to other isoforms of CA, and even other enzymes of therapeutic interest such as matrix metalloproteinases or serine hydrolases. Targeting these enzymes will help us understand how we can inhibit them as well as dilucidate their roles in disease This study demonstrates the potential that lies in increasing experimental throughput of CuAAC and harnessing the possibilities that noncanonical amino acids open for protein engineering.